GENERATION OF 1.55 MICRON PULSED FIBRE LASER USING GRAPHENE OXIDE AND ZINC OXIDE AS A SATURABLE ABSORBER

NUR'AFIQAH BINTI ABDUL AZIZ

DISSERTATION SUBMITTED IN FULFILMENT OF THE REQUIREMENTS FOR THE DEGREE OF MASTER OF ENGINEERING SCIENCE

FACULTY OF ENGINEERING
UNIVERSITY OF MALAYA
KUALA LUMPUR

2019

UNIVERSITY OF MALAYA

ORIGINAL LITERARY WORK DECLARATION

Name of Candidate: Nur'Afiqah binti Abdul Aziz

Registration/Matric No: KGA150069

Name of Degree: Master of Engineering Science

Title of Project Paper/Research Report/Dissertation/Thesis ("this Work"):

Generation of 1.55 micron pulsed fibre laser using Graphene Oxide and Zinc Oxide as a saturable absorber

Field of Study:

I do solemnly and sincerely declare that:

(1) I am the sole author/writer of this Work;
(2) This Work is original;
(3) Any use of any work in which copyright exists was done by way of fair dealing and for permitted purposes and any excerpt or extract from, or reference to or reproduction of any copyright work has been disclosed expressly and sufficiently and the title of the Work and its authorship have been acknowledged in this Work;
(4) I do not have any actual knowledge nor do I ought reasonably to know that the making of this work constitutes an infringement of any copyright work;
(5) I hereby assign all and every rights in the copyright to this Work to the University of Malaya ("UM"), who henceforth shall be owner of the copyright in this Work and that any reproduction or use in any form or by any means whatsoever is prohibited without the written consent of UM having been first had and obtained;
(6) I am fully aware that if in the course of making this Work I have infringed any copyright whether intentionally or otherwise, I may be subject to legal action or any other action as may be determined by UM.

Candidate's Signature Date:

Subscribed and solemnly declared before,

Witness's Signature Date:

Name:

Designation:

ABSTRACT

This research work aims at exploring various new materials for saturable absorber (SA) application in generating Q-switching pulses train operating at 1.5 μm region. These nanomaterials are graphene oxide (GO) and zinc oxide (ZnO). The fibre lasers employ Erbium-doped fibre (EDF) as an amplification medium. Firstly, passive Q-switched Erbium Doped Fibre Lasers (EDFLs) have been successfully demonstrated using the newly developed GO film based SAs based on two different host polymers; Poly (Vinyl alcohol) (PVA) and Poly (Methyl methacrylate) (PMMA). The GO material was obtained through chemical oxidation of graphite. By incorporating GO PMMA SA into an EDFL set up, sturdy Q-switched pulses train were generated to operate in a wavelength of 1531.6 nm as the pump power being tuned within vary of 11.8 to 83.0 mW. The repetition rate was tunable within 21.5 kHz to 68.7 kHz. The maximum pulse energy of 145 nJ and the minimum pulse duration of 6.12 μs were obtained at the pump power of 83.0 mW. The research proceeds with the GO PVA SA, where the Q-switched was realized with the repetition rate tunable from 32.45 kHz to 81.7 kHz. At the maximum pump, the highest single pulse energy and repetition rate of 109.30 nJ and 81.7 kHz were achieved. These results show that GO PMMA film operate excellent than PVA film in terms of operating pump power range and pulse energy. Later, two Q-switched EDFLs were also proposed and demonstrated using a ZnO based SA. It is worthy to note that the EDFL produces a stable Q-switched pulses train with a higher pulses energy when the polymer material was replaced from PMMA to PVA. The ZnO PVA film-based Q-switched laser operated at 1560.4 nm within the 980nm pump power range from 11.8 mW to 77.9 mW. At 77.9 mW pump power, the laser showed the repetition rate, pulse energy, and pulse duration of 61.43 kHz, 154.6 nJ, and 7.00 μs, respectively. These results show that both GO and ZnO materials have new potential for application in pulsed laser generation.

ABSTRAK

Kajian ini tertumpu pada penerokaan pelbagai bahan baru untuk aplikasi penyerap tertepu dalam menjana denyutan suis Q yang berterusan dan beroperasi dalam lingkungan 1.5 μm. Bahan nano yang digunakan adalah grafen oksida (GO) dan zink oksida (ZnO). Gentian terdop Erbium digunakan di dalam gentian laser sebagai medium gandaan. EDFL pasif suis Q telah di demonstrasi, dengan menggunakan GO filem SA baru yang di hasilkan dari dua jenis polimer sebagai bahan filem iaitu '*Poly (Methyl methacrylate)*' (PMMA) dan '*Poly (Vinyl alcohol)*' (PVA). Bahan GO diperolehi hasil daripada pengoksidaan kimia grafit. GO PMMA SA telah menghasilkan denyutan suis Q yang stabil dan beroperasi di 1531.6nm apabila kuasa pam dilaraskan dalam anggaran 11.8 sehingga 83.0 mW. Kadar pengulangan denyutan boleh diubah diantara 21.5 kHz ke 68.7 kHz. Nilai maksimum tenaga denyutan 145 nJ dan tempoh masa denyutan minima 6.12 μs diperolehi apabila pam kuasa dilaraskan pada 83.0 mW. Kajian ini diteruskan dengan GO PVA SA dimana suis Q telah direalisasikan dengan kadar pengulangan yang boleh diubah dari 32.45 kHz kepada 81.7 kHz. Pada nilai maksimum pam, kadar pengulangan tertinggi dan tenaga denyutan tunggal sebanyak 81.7 kHz dan 109.30 nJ telah dicapai. Hasil kajian ini menunjukkan bahawa filem GO PMMA berinteraksi lebih baik berbanding PVA dari segi julat pam kuasa beroperasi dan tenaga denyutan. Selain itu, dua suis Q EDFL juga telah dicadangkan dan ditunjukkan menggunakan SA berasaskan ZnO. EDFL telah menghasilkan denyutan yang berterusan dengan tenaga denyutan yang tinggi apabila bahan polimer diganti dari PMMA ke PVA. Laser suis Q berasaskan filem ZnO PVA beroperasi pada 1560.4 nm dalam julat kuasa 980 nm dari 11.8 mW sehingga 77.9 mW. Pada pam kuasa 77.9 mW, laser telah menunjukkan kadar pengulangan, tenaga denyutan dan tempoh denyutan sebanyak of 61.43 kHz, 154.6 nJ, dan 7.00 μs. Keputusan kajian ini menunjukkan bahawa kedua-dua bahan GO dan ZnO berpotensi untuk menjadi bahan baru dalam aplikasi yang memerlukan penjanaan denyutan laser.

ACKNOWLEDGEMENTS

First of all, I would like to express my thankfulness and gratitude to Allah S.W.T who has given me all the strength that I needed to prepare this report. I also want to give my deepest appreciation to my supervisor, Dr. Effariza binti Hanafi and my co-supervisor, Professor Dr. Sulaiman Wadi Harun. I really appreciate their tips and guidelines that give me pleasure to solve this project. Without their assistance and dedicated involvement in every step throughout the process, this dissertation would have never been accomplished. I would like to thank you very much for your support and understanding over this past whole semester. Through them, I gain a lot of experience and knowledge that may never be acquired elsewhere.

I really want to give my thanks to the entire friend that help me in providing the knowledge and led me to finish the research. Without their supported and time that they take to help me, it is impossible to finish this dissertation. They are the one that is around me during the whole time while I conducted this research and incanted me to strive towards my goal. I am really do appreciated it

I also want to give a special thanks to my family. Words cannot express how grateful I am to my mother Anita binti Anoh, my father Abdul Aziz bin Shaikh Ahmad Ishak and my siblings for all of the sacrifices that they have made on my behalf. Your prayer for me was what sustained me this far. My mother and my father that always call and support me with their word and idea. The spirit that they give and always stand by my side was really helping me. Without everyone, I am only just a piece of white sheet paper and because of them, I can be a beautiful painting as I am right now. I still hope their guide in the future.

TABLE OF CONTENTS

LIST OF FIGURES

LIST OF SYMBOLS AND ABBREVIATIONS

ASE	:	Amplified Spontaneous Emission.
$(CH_2)N_4$	:	Hexamethylenetetramine
CNT	:	Carbon Nanotubes
CO_2	:	Carbon Dioxide
Co_3O_4	:	Cobalt Oxide
CW	:	Continuous Wave
DI	:	Deionized Water
EDF	:	Erbium Doped Fibre
EDFA	:	Erbium Doped Fibre Amplifier
EDFL	:	Erbium Doped Fibre Laser
eV	:	Electron Volt
FBG	:	Fibre Bragg Grating
FC/PC	:	Ferrule Connector / Physical Contact
FESEM	:	Field Emission Scanning Electron Microscopy
GO	:	Graphene Oxide
HCL	:	Hydrochloric Acid
H_2O_2	:	Hydrogen Peroxide
H_3PO_4	:	Phosphoric Acid
H_2SO_4	:	Sulfuric Acid
$KMnO_4$	:	Potassium permanganate
LASER	:	Light Amplification by Stimulated Emission of Radiation
LASIK	:	Laser- Assisted In Situ Keratomileusis
LED	:	Light Emitting Diode
MCVD	:	Modified Chemical Vapor Decomposition

MoS_2	:	Molybdenum Disulfide
NA	:	Numerical Aperture
NPR	:	Nonlinear Polarization Rotation
O^{2-}	:	Oxygen ion
OSA	:	Optical Spectrum Analyzer
PMMA	:	Poly(methyl methacrylate)
PVA	:	Poly (vinyl alcohol)
RF	:	Radio Frequency
SA	:	Saturable Absorber
SBS	:	Stimulated Brillouin Scattering
SESAM	:	Semiconductor Saturable Absorber Mirrors
SMF	:	Single Mode Fibre
SNR		Signal to Noise Ratio
SPM	:	Self-Phase Modulation
TiO_2	:	Titanium Dioxide
Tm^{3+}	:	Thulium ion
TMDs	:	Transition-metal Dichalcogenides
TPA	:	Two-Photon Absorption
UV	:	Ultra Violet
WDM	:	Wavelength Division Multiplexer
Yb^{3+}	:	Ytterbium ion
Zn^{2+}	:	Zinc ion
ZnO	:	Zinc Oxide
$Zn(NO_3)_2 \cdot 6H_2O$	:	Zinc Nitrate Hexahydrate
3D	:	3 Dimensional

CHAPTER 1:

INTRODUCTION

1.1 Introduction to Fibre Laser

The optical waveguide was first demonstrated in 1854 when John Tyndal proves the total internal reflection concept. In the experiment, he proved that the light signal could be bend by using a tank of water with a pipe. When he shone a light into the tank, the light was projected into the stream of water. Optical fibre operates based on the total internal reflection principle to propagate light. As the time past, optical fibre technology becomes more advanced and developed a revolution to the telecommunication industries. Besides telecommunications, optical fibre also has been applied in many areas including materials processing, telecommunications, spectroscopy and medicine (Bouma et al., 1998; Henderson et al., 1993; Liu, Wang, & Wang, 2012; Gary D Spiers et al., 2011).

The optical fibre applications become more widely explored with the invention of the LASER (Light Amplification by Stimulated Emission of Radiation) in the early 1960s. LASER produces a powerful coherent light that gives the possibility to modulate at a high speed compared to sunlight and Light Emitting Diode (LED). The laser is broadly classified into various types according to their active media such as gas lasers (CO_2 laser), liquid lasers (dye laser) and solid-state lasers (semiconductor lasers and fibre lasers). However, fibre lasers are preferred compared to other sort of lasers because of their advantages in terms of reliability, compactness, zero alignments and low cost (Dong & Samson, 2016). Furthermore, they can provide high output and peak power. Since the gain medium is formed of an optical fibre, it can also be easily integrated into the optical communication system with the lowest possible coupling loss. Due to these merits, fibre lasers become essential devices in many engineering fields including metal cutting and

folding, laser welding, 3D printing, optical communications and spectroscopy. Optical lasers also have become an important apparatus in the applications of optical sensors, industry, medicine and military (Fermann, Galvanauskas, & Sucha, 2002)

Fibre lasers can operate in various ranges of wavelengths depending on the type of the rare earth material that used in doping of the fibre. The most common active materials that being used are ytterbium, erbium, thulium, which operates in 1μm, 1.5μm and 2μm wavelength regions, respectively. Although there has various type of rare earth material, erbium doped fibre lasers (EDFLs) are the most developed fibre lasers where they gained tremendous interest, especially for sensing and optical communication applications. Normally, fibre lasers can operate in two types of the waveform which is a continuous wave (CW) or pulsed modes. However, the main reasons pulsed lasers have gained more intentions in nowadays are due to their wide scope of applications including laser surgery, industrial, range finding, optical communication and fibre sensing.

Pulsed fibre lasers can be obtained by either Q-switching or mode looking mechanisms. Q-switching is used to produce short pulses of light with high peak power, which is higher than that could be produced by similar laser operates in CW mode through the modulating of the loss inside the laser cavity. On the other hand, mode-locking can be used to produce ultrafast pulses of light with much higher peak power than the Q-switching technique through the locking of the oscillating modes inside the laser cavity. Recently, Q-switched fibre laser has drawn increasing research attention for applications that require high pulse energy at the moderate pump power. Therefore, this study aims to develop a Q-switched fibre laser using new passive techniques.

1.2 Problem Statement and Motivation of the Study

Passively Q-switched fibre lasers have captivated a lot of attention in the past few years due to their ability to operate in various fields such as medicine, metrology, fibre optical sensing, telecommunications and micromachining (Hendow & Shakir, 2010; Wood, Plunkett, Previn, Chidlow, & Casson, 2011). Passive Q-switched are finer than active Q-switched due to its flexibility during implementation, and the circuit is compact but uncomplicated (Shi-Xiang, Wen-Xue, Qiang, Hui, & He-Ping, 2008).

Two types of mechanism can be used to realise the passive Q-switching which is nonlinear polarisation (NPR) (Z. Zhang, Sang, Ye, & Nie, 2008) or saturable absorber (SA). Today, numerous SAs have been fabricate such as carbon nanotubes (CNT) (S. Harun et al., 2012), semiconductor saturable absorber mirrors (SESAMs) (L. Zhang et al., 2010), and graphene (Yap, Richard, Pua, Harun, & Ahmad, 2012) to generate Q-switching pulse that operate in multi-cavities and fibre lasers. The SAs known as SESAM is famous due to its ability to generate a stable pulsed. However, the fabrication of SESAMs require complex procedures, which prompt economic inefficiency. Besides being expensive, the operation of SESAMs is limited by their narrow bandwidth operation (Keller, 2003).

On the other hand, CNT tends to have large non-saturable losses because of the broad diameter distribution (Hisamuddin et al., 2016). Graphene possesses advantages in ultrafast recovery time and broadband saturable absorption, but it shows weak modulation depth and the difficulty of forming an optical bandgap. Therefore, there are many new attempts in recent years to develop new high-performance SAs for Q-switching laser operation (Ahmad, Reduan, et al., 2016; Jagadish & Pearton, 2011; Janotti & Van de Walle, 2009; Reynolds, Look, & Jogai, 1996).

The transition-metal dichalcogenides (TMDs) were also extensively studied in recent years as a SA for generating Q-switched pulse in fibre laser (Chen et al., 2013; Q. H. Wang, Kalantar-Zadeh, Kis, Coleman, & Strano, 2012). For instance, molybdenum disulfide (MoS_2) based Q-switched lasers have been demonstrated due to their thickness dependent band-gap and unique absorption property (Hisamuddin et al., 2016). However, its fabrication process is complicated.

Likewise, other nanomaterials such as zinc oxide (ZnO) (Jagadish & Pearton, 2011) and titanium dioxide (TiO_2) nanoparticles (Ahmad, Reduan, et al., 2016) were also reported as SA, where they are functioning as good as the conventional material. In general, an ideal SA material should have a broadband absorption, appropriate modulation depth, low saturation intensity, ultrafast recovery time, and high damage threshold.

Recently, graphene has become one of the most massive and promising materials as a saturable absorber (Yap et al., 2012). Graphene can be obtained from carbon and have excellent optical characteristics, such as high saturable absorption rates and ultra-fast recovery times. Both this material is significantly easier, and the cost is cheap as compare to the SESAM and other materials.

Likewise, the interest in Zinc Oxide (ZnO) is growing in more recent years due to its optical properties that complementary to graphene. ZnO has been clearly explored due to its outstanding features such as its similar band gap to TiO_2, low cost, chemical stability and non-toxicity (Hassan, Hashim, & Al-Douri, 2014; Jimenez-Garcia, Londono-Calderon, Espinosa-Arbelaez, Del Real, & Rodriguez-Garcia, 2014; Xu & Wang, 2011). ZnO is also an important semiconductor material with an expansive band gap of 3.3 eV and abundant exciton binding energy of 60 meV (Jagadish & Pearton, 2011)

which extensively been used in the optoelectronic instruments such as photodetectors for UV spectral range and laser diodes (Reynolds et al., 1996).

In this dissertation, passively Q-switched EDFLs are proposed and demonstrated using graphene oxide and ZnO as a saturable absorber (SA). The SA is integrated with the EDFL cavity by sandwiched the thin film of graphene oxide or ZnO between two fibre ferrules to achieve a stable pulse train with a good repetition rate, pulse width and peak power. The performance of both lasers is compared and discussed in this dissertation.

1.3 Objectives

The research work aims to demonstrate Q-switched EDFL using two types of nanomaterials as SAs; graphene oxide and zinc oxide. This research embarks on the following objectives:

i) To prepare and characterise graphene oxide SAs, which were obtained by embedding the nanomaterial inside Poly (Vinyl alcohol) (PVA) polymer and Poly (Methyl methacrylate) (PMMA) polymer.

ii) To prepare and characterise ZnO SAs, which were obtained by embedding the nanomaterial inside Poly(Vinyl alcohol) (PVA) polymer and Poly (Methyl methacrylate) (PMMA) polymer.

iii) To demonstrate the generation of Q-switching pulses using GO PMMA, GO PVA, ZnO PMMA and ZnO PVA based SAs in EDFL cavity

1.4 Outline of the Dissertation

This dissertation provides an in-depth description and analysis of the experimental work on Q-switched EDFLs using two different materials (GO and ZnO) as SAs. This research work focuses on investigating the performance of the newly developed passive SAs based on GO and ZnO materials. These materials are embedded into two types of polymers; PMMA and PVA and incorporated into an EDFL cavity to generate Q-switching pulses operating at 1550 nm region. The content of this dissertation is arranged in 5 chapters, including this introductory chapter and conclusion chapter. Chapter 1 explained the motivation and objectives of this research work. An in-depth review on optical fibre, laser, Q-switching, saturable absorber, graphene oxide and zinc oxide are presented in Chapter 2. Chapter 3 demonstrates a Q-switched EDFL based on a new GO material as SA. The SA device is fabricated by embedding a graphene oxide material, which was obtained through chemical oxidation of graphite into two types of polymer which is PVA and PMMA film. Due to the unselective absorption of graphene absorber, it can be applied in a broad wavelength range. A stable and high-power Q-switching pulses are obtained by incorporating a small piece of the film in a laser cavity. Chapter 4 proposes and demonstrates two Q-switched EDFLs using a ZnO powder as a base material for a SA. At first, the SA is fabricated by embedding the prepared ZnO powder into PMMA film. By incorporating a small piece of the film in a laser cavity, the proposed laser is able to generate a stable Q-switched pulses train at 1559.3 nm with repetition rate rises from 24.85 to 85.91 kHz. Besides, the pulse width reduces from 17.88 to 4.66 μs as the pump power was increased from 12 to 98.49 mW. By replacing the polymer material from PMMA to PVA, the EDFL generates a stable Q-switched pulses train with greater pulse energy.Finally, Chapter 5 concludes the finding of this research by summarising the overall work. It also describes the possible future work based on the results of this research.

CHAPTER 2:

LITERATURE REVIEW

2.1 Introduction

Fibre lasers have a broad range of applications ranging from industry to optical communication. Many laser setups produce a pulse with different and distinctive pulse characteristics. Therefore, each laser setup can be designed to accommodate for a specific type of applications. For example, in the electronic and automotive industry, Q-switched laser is suitable for micromachining and drilling due to its high peak intensity and high pulse energy (Nikumb et al., 2005). In addition, Q-switched lasers are beneficial in the medical fields, in particular, eye (Plamann et al., 2010) and dental surgery (Serbin, Bauer, Fallnich, Kasenbacher, & Arnold, 2002). One of the eye surgery methods that use the application of a pulse laser is Laser-assisted in situ keratomileusis (LASIK) (Kezirian & Stonecipher, 2004).

There are two techniques to generate Q-switched fibre laser which are active or passive techniques. The active technique is usually realised by integrating an external controller device like acoustic-optic modulator to actively modulate the light of the intracavity (Bello-Jimenez et al., 2010). On the opposite side, the passive technique utilises saturable absorption of optical material to change the intra-cavity light and generates a pulsed laser in the cavity (De Tan et al., 2010).

Passive Q-switching laser operation depends on the gain medium as well as the saturable absorber (SA) which acts as a Q-switcher, and it occurs when the photon flux starts to show a fixed loss, saturable loss as well as gain in the SA after many roundtrips. Up to now, many passive methods are proposed to generate Q-switched fibre lasers.

Therefore, this study aimed to demonstrate Q-switched fibre lasers, which operate in the 1.5-micron region using new types of SAs. This chapter provides a comprehensive review on numerous topics on fibre lasers, in particular, optical fibres, Erbium-doped fibre, Q-switching, SA, graphene oxide and Zinc Oxide materials.

2.2 Optical Fibre

John Tyndall states that the light signal can be bend, however, there also will have a loss during light transmission since light can be pass through the air. Silica glass is the first item that is invented to trap a light signal, but since it is surrounded by air, there have some excessive losses at any discontinuities of the glass-air interface. To solve this problem, a researcher has invented a transparent layer to wrap a silica core. The wrap is known as cladding. Cladding is invented to support the core where the cladding will have a slightly lower refractive index as compared to the core. Therefore, when light transmits, it will travel in the core and substantially reducing the radiation loss into the surrounding air. Up to date, there have several types of fibre optic in the industry, however, the basic type of fibre optic is single mode and multimode.

Figure 2.1 describes the schematic diagram of both single-mode and multimode fibre structures. The significant difference between multimode and single mode is the diameter of the core. Single mode has a small core which is about 9 microns in diameter where it can transmit infrared laser at the wavelength of 1300nm to 1550nm while multimode consist of a larger core that is about 62.5 microns where it can transmit a wavelength 850nm to 1300nm. As shown in Figure 2.1, the single mode can only carry one and travels as a straight line at the core's centre. However, for multimode, at a specific wavelength, it can carry more than one mode. In this research work, all fibres used are single mode fibre (SMF). SMF has become focused on the researcher because it can cover

a larger bandwidth and higher information rate. SMF also is more convenient to use in long distances applications such as telecommunication.

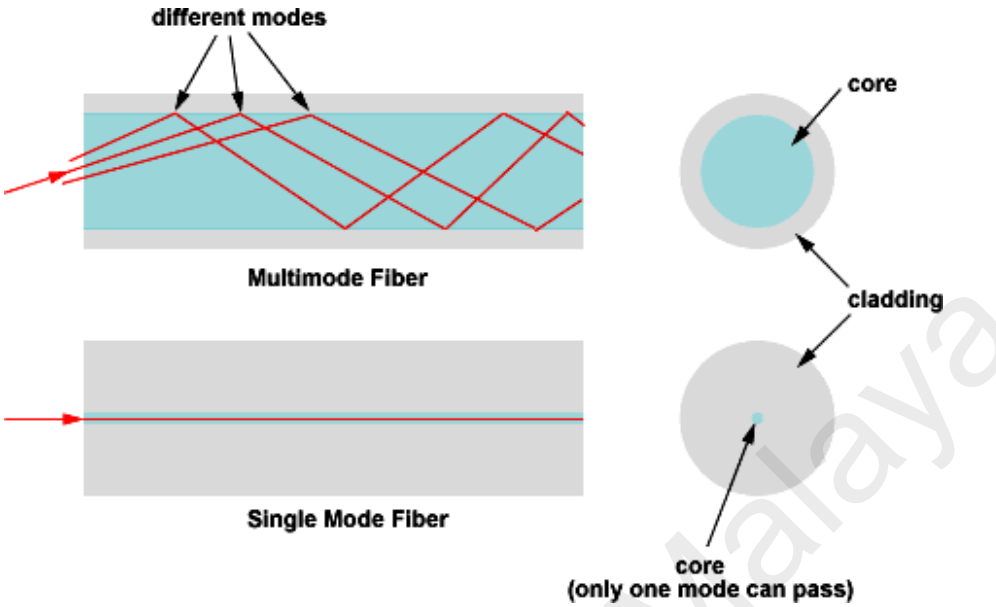

Figure 2.1: Optical fibre structures with the array pathway

2.3 Erbium-doped fibre

Fibre lasers use an optical fibre, which is doped with active rare-earth ions as a gain medium. Rare-earth ions are shown as lanthanides series of chemical elements in the periodic table. Various type of rare-earth ions has been used in fibre lasers such as Neodymium, Ytterbium, Thulium, Praseodymium, Erbium and Holmium. During a decade ago, the rare-earth ion is doped with a fibre optic by using a modified chemical vapour decomposition (MCVD) technique. This technique provides a low background loss in the fibre optic. The erbium ions are the most desirable rare earth element for optical communication applications. This attributed to the Erbium gain, which falls in the third communication window where the loss in the optical fibre is lowest. Since the first fabrication in 1978 (Mears, Reekie, Jauncey, & Payne, 1987), EDFs have been intensively studied and used for construction of erbium-doped fibre laser (EDFL) and

erbium doped fibre amplifier (EDFL) (Desurvire, Giles, Simpson, & Zyskind, 1991; Mizrahi et al., 1993). EDFs attract the worldwide interest from its ion that gives a promising transition at 1.5 μm which is suitable to act as an amplifying medium in the latest transmission system in fibre optic. High signal gains obtained when the first demonstration of single mode EDF by using both argon laser-pumped dye laser (650 nm) and an argon laser (514 nm) are conducted(Becker, Olsson, & Simpson, 1999). Figure 2.2 illustrates the energy level diagram of the erbium ions showing many exciting levels. This indicates that erbium ions can be pumped with many different wavelengths, which is equivalent to the difference of energy between the excited level and the ground state (Laming et al., 1989). However, 1480 nm and 980 nm are the most appropriate wavelengths because they are the fewer energies that could be used to excite erbium ions.

As erbium ions are pumped with 1480 nm photons, they will be excited from the ground state $^4I_{15/2}$ directly to the metastable level $^4I_{13/2}$. Then within the group of levels of $^4I_{13/2}$ rapid relaxation would occur to the lowest sub-level where laser action would take place. Therefore, in this case, it is called two levels system owing to only two energy levels are involved in the overall process. However, if erbium ions pumped with 980 nm, they will be excited from the ground state $^4I_{15/2}$ to higher unstable excited state $^4I_{11/2}$ where they will stay for a very short time of approximately one μs before they decay to the lower metastable level $^4I_{13/2}$ through releasing heat. So, it is a non-radioactive transition. As a result, population inversion will be achieved between the metastable level and the ground state. Finally, after spending their lifetime they will make a transition to the ground state through either spontaneous emission or stimulated emission. With 980 nm pumping, it is referred to three levels system owing to the three energy levels are involved in the overall process. Despite the optical power conversion efficiency of the 1480 nm pumping is higher than that of 980 nm pumping, yet the latter is highly preferred and commonly used due to its many advantages such as low noise, larger population inversion and wider

separation between the laser wavelength and pump wavelength (El-Mashade & Mohamed, 2017).

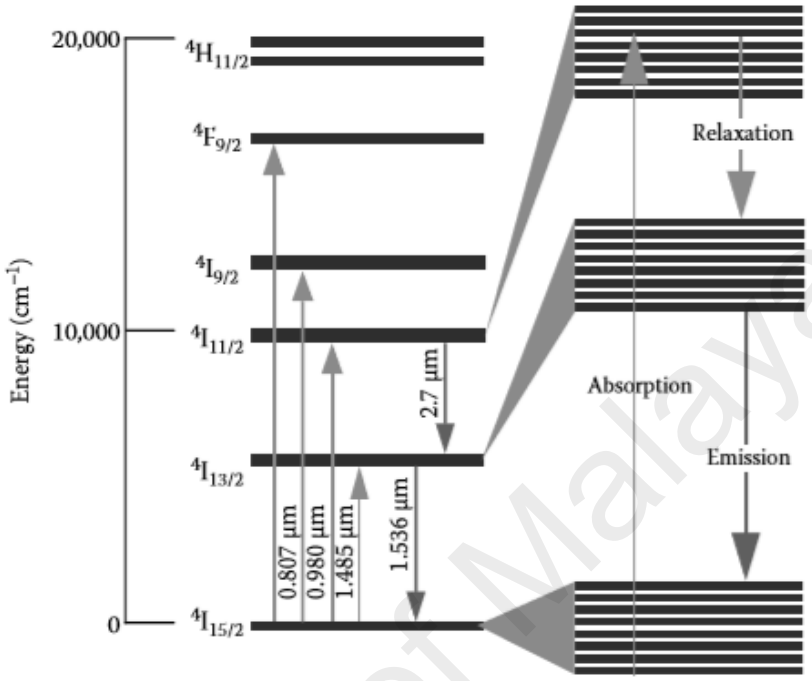

Figure 2.2: Energy level diagram for Erbium ions (Ngo, 2010)

The process to emit energy in the form of a photon can be divided into two ways; spontaneous emission and stimulated emission. In spontaneous emission, the process will start when 980 nm laser diode is launched into the EDF. During 980 nm pumping, the Erbium ions in the fibre will be excited and move from the grounds state to excited state. However, the ions will be fast decay to the meta-stable state because it is unstable. During this stage, no photon will be emitted even if the ions are pump because it is known as a non-radioactive decay. The ions will drop down and emit the photons when the photon is in the right amount. Every ion that emits with the incident photon will produce another photon that is called as the emitted photon. The process during this transition is called spontaneous emission. The photon wavelength that is produced in the spontaneous emission is in the range of 1520nm to 1570nm. Since the emitted photon has the same

phase and wavelength as the incident photon, it can reflect into an amplifying medium to excite the ions. During spontaneous emission, the photon will be amplified as it propagates in the fibre and the output light from the EDF is referred to as amplified spontaneous emission (ASE).

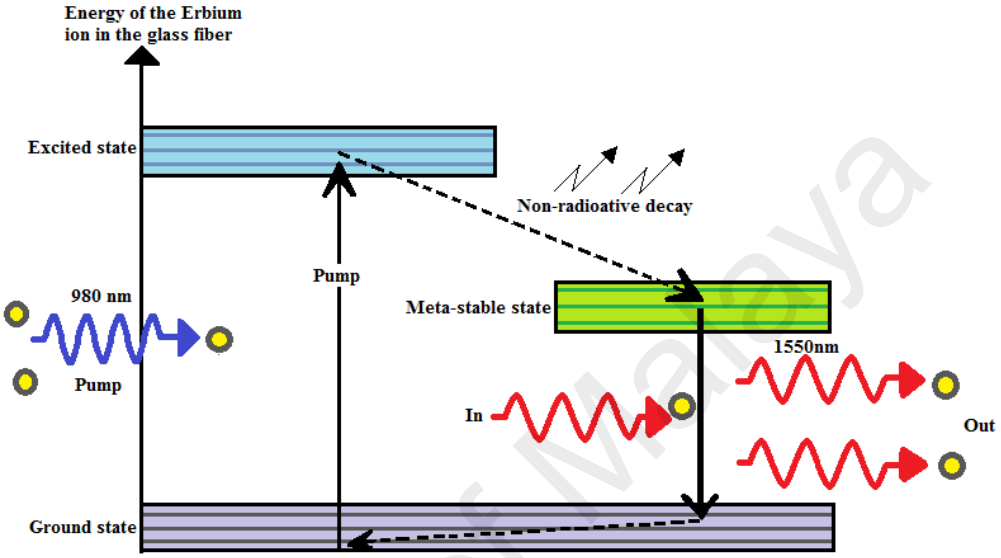

Figure 2.3: The process during spontaneous emission and stimulated emission

2.4 Q-switching

Q-switching is a technique to generate intense short pulses of light using a laser. The basic principle is as follow: In the first phase, the gain medium is pumped. By keeping the resonator losses high (in other words, the Q factor is kept low), the extraction of energy as laser light is prevented. It can be achieved using active or passive techniques. Then, the resonator losses decrease suddenly. The interactivity power increases exponentially (usually starts from weak fluorescence light of the gain medium) when the gain is substantially greater than the resonator losses. When the gain is saturated, the power decreases again.

The light pulse that is generated can extract a huge percentage of the energy that was originally stored in the gain medium. For high pulse energy, the gain medium must have a high-energy storage capability, where the upper-state lifetime is long, the density of laser-active ions or atoms is high and gain efficiency that is not too high. The latter is vital since amplified spontaneous emission could otherwise limit the stored energy and produce a huge initial loss that is required to prevent premature lasing.

Active Q-switching, which is based on active loss modulation, is usually achieved by incorporating an acousto-optic modulator into the laser resonator. The modulator produces huge losses, which then leaves the resonator. These losses are generated by diffraction into the first-order beam when the RF power is applied to the modulator. By suddenly switching off the RF power, the pulse is triggered. The gain medium is continuously pumped, and the Q-switch is triggered repetitively for high pulse repetition rates. A passive Q-switching is realised by incorporating an optical element, like a doped crystal, a cell filled with organic dye or a passive semiconductor device. The characteristic of such material is that when the light intensity exceeds a certain threshold, the transmission increases. Laser oscillation could initially be prevented if a material with high absorption at the laser wavelength is placed inside the laser resonator. As the gain rises significantly, it causes the passive Q-switch to saturate. The losses are low under this condition and a Q-switch pulse builds up.

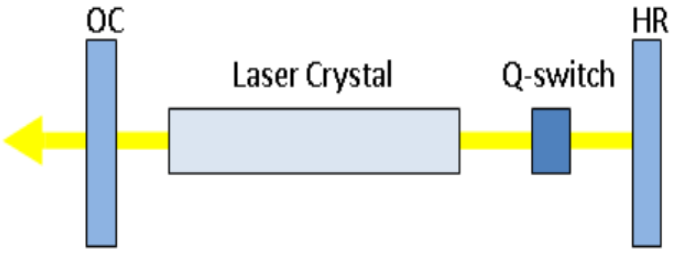

Figure 2.4: Simple concept of a solid-state laser with a passive Q-switching technique (Kozinc, 2015)

The Q-switching technique was first described in 1961 by Hellworth where he proposed that laser could produce short pulses if the cavity loss is switching suddenly. Therefore, Q-switching is defined as a method of producing extremely short pulses of light with high peak power, which is greater than CW mode in a fibre laser. Based on a theory, a variable attenuator which is commonly known as “Q switcher” is place inside the laser’s cavity to generate Q-switching. When this attenuator operates, lasing will not occur due to the light inside the cavity are unable to oscillate and causes the decreasing in the quality factor or Q factor of the cavity. Low Q factor will correspond to high cavity loss per round trip and vice versa (Ahmed, 2015). This process is illustrated in Figure 2.5. The Q-switching can be achieved either actively or passively based on the variable attenuator used. If the Q switcher is an active element; for instance, acoustic-optic modulator or electro-optic modulator, the Q-switching produced is active. While if the Q-switcher used is a passive element such as saturable absorber (SA), the Q-switching generated is passive. The passive Q-switching techniques are preferred over the active one because they got the advantages of simplicity, more stable and low cost (Ahmed, 2015).

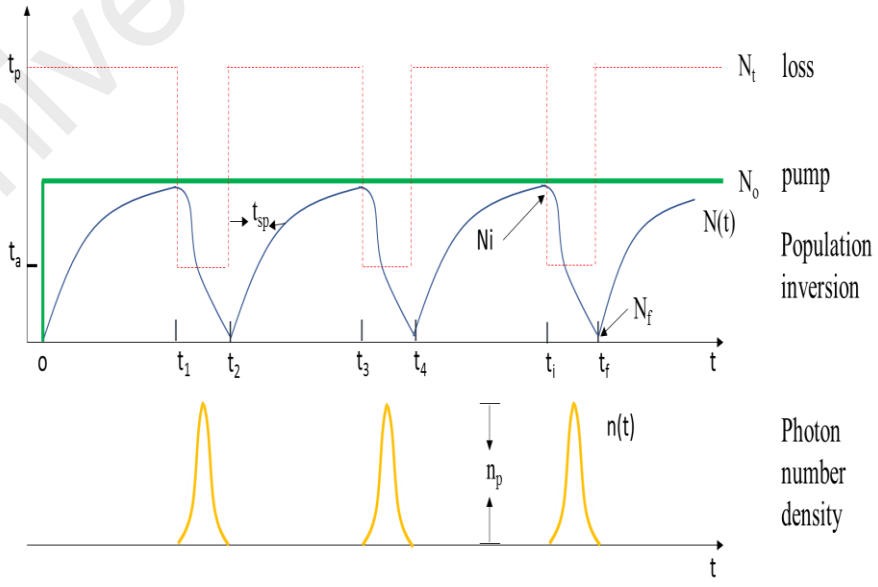

Figure 2.5: Passive Q-switching operation

Various techniques could be employed to produce a Q-switched EDFL. Passive Q-switching could be realised by using a saturable absorber based on a segment of Yb^{3+} -doped Tm^{3+} co-doped fibre (Adel et al., 2003). Q-switched EDFL can also be generated using Stimulated Brillouin Scattering (SBS) in the fibre, as in (Fotiadi, Deparis, Kiyan, Chernikov, & Ikiades, 2000). On the other hand, active Q-switching can be generated by using an electro-optic modulator (Alvarez-Chavez et al., 2000), or acousto-optic modulator (Alvarez-Chavez et al., 2000; Y. Wang, Martinez-Rios, & Po, 2003). Recently, some all fibre methods based on different modulation techniques as intensity modulators (Chandonnet & Larose, 1993), and acousto-optic attenuators (Huang, Liu, & Yang, 2000) have been reported. Q-switching of all-fibre lasers by tuning FBGs using piezoelectric (Russo, Duchowicz, Mora, Cruz, & Andrés, 2002)or modulating with an extensional acoustic wave (M Delgado-Pinar, Zalvidea, Diez, Pérez-Millán, & Andrés, 2006) and magnetostrictive transducers (Pérez-Millán, Díez, Andrés, Zalvidea, & Duchowicz, 2005) have been demonstrated.

2.5 Saturable Absorber

Saturable absorbers (SAs) are a nonlinear optical material with an optical loss, and this loss decreases at a high intensity of light. In a gain medium with absorbing dopant ions, for instance, the optical loss could happen when a strong optical intensity leads to depletion of the ground state of these ions.

Usually, the saturable absorber will have a low saturation intensity, which can be assumed as a two-level process. The SA will hold the photons until it's saturated in a low-incident light intensity and bleach until it becomes almost transparent. During transparent, the photon will pass through the SA. The SA become unsaturated again as the photon is

low (Svelto, 1998). Therefore, SA loss properties will determine the modulation depth and the minimum pulse width that can be generated.

Since parameters of SAs would vary depending on their intended applications, different devices are used:

a) Semiconductor saturable absorber mirrors (SESAMs) are frequently used (Keller et al., 1996) for passive mode locking as well as Q-switching. It could also be used for passive Q-switching, especially at lower pulse energies.

b) Thin layers of carbon nanotubes (CNTs) and single-wall nanotubes have been used for mode locking of lasers (Schmidt et al., 2008; Set, Yaguchi, Tanaka, & Jablonski, 2004; Shohda, Shirato, Nakazawa, Komatsu, & Kaino, 2008). These absorbers are desirable for broadband lasers as they can exhibit very broadband absorption features. High pulse repetition rates could be obtained by applying thin layers of the nanotube to fibre ends and use them mode locking of very compact fibre lasers (Martinez & Yamashita, 2011). Although the recovery time of nanotube absorbers is quite short, for some applications, significant non-saturable losses could cause a problem.

c) SAs materials are used in the form of optical fibre in a rare case. For instance, chromium, samarium or bismuth dopants can serve this function in Q-switched fibre lasers (Dvoyrin, Mashinsky, & Dianov, 2007).

Selecting a suitable SAs depends greatly on the concrete circumstances on the desired properties of a SAs. For a passively Q-switched laser, the requirements on a SA are as follows:

i. If high pulse energy and short pulse duration are desired, the total non-saturated absorption must be relatively high, which is often slightly lesser than the small-signal gain of the laser medium.

ii. To minimise the power losses, low saturation fluence and low non-saturable losses are preferred.

iii. The recovery time should not be too long (even though this problem rarely occurs). In contrast, ideally, it should not be shorter than the pulse duration. However, the latter condition is often not crucial, especially when the saturation fluence is way below the pulse fluence.

iv. Sufficiently high damage threshold in terms of intensity and fluence.

In general, the parameters of the absorber should be chosen based on the comprehensive laser design processes, which considers both the dynamics of pulse generation as well as the limitation of the absorber tolerance to high intensities or pulse energies.

2.6 Graphene Oxide

Graphene is a material that is made from carbon atoms which are bonded together in a repeating pattern of hexagons as illustrated in Figure 2.6. Graphene is considered as two dimensional because it is thin. Graphene's flat honeycomb shape provides various remarkable characteristics, for example, the most durable material as compared to other materials, lightest weight, flexible, most conductive as well as transparent. As such, graphene has brought substantial potential applications in various industries, in particular, electronics, medicine, and aviation. Graphene has high transparency, which is near to 97.7% and low absorption light (2 %) make it one of the most suitable SA in the fibre optic laser. The single layer of carbon atoms gives various other materials. For instance, the substance found in pencil lead, which is Graphite, is formed by stacked graphene. Besides that, carbon nanotubes which are made of rolled graphene and are used in many emerging applications. The improvement of the GO change its optical properties in absorption

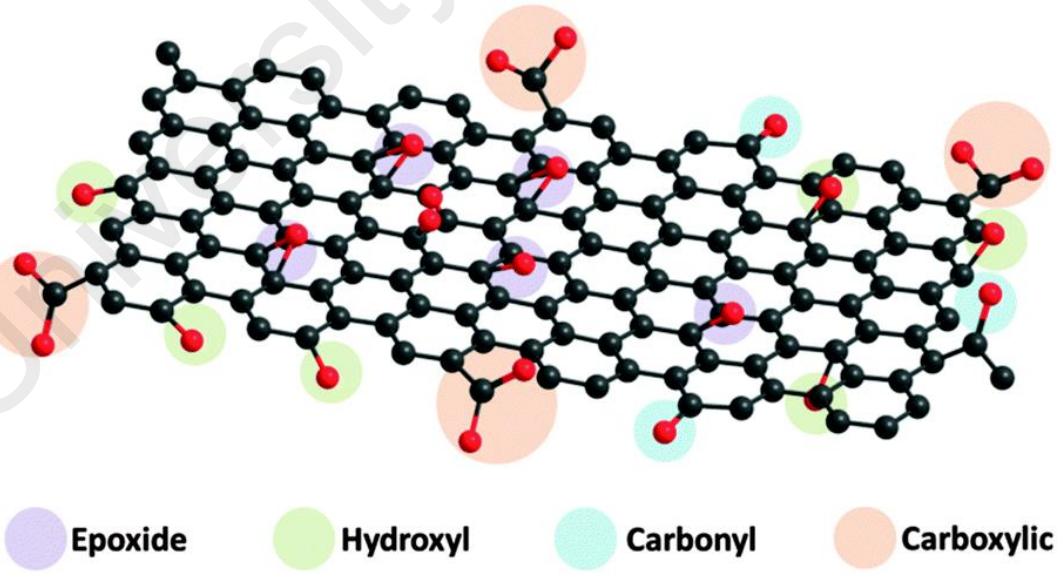

Figure 2.6: GO structure atom

Since graphene is costly and relatively challenging to produce, great deals are made to search for cheaper and effective ways to produce and make use of graphene derivatives or related materials. By using a powerful method of oxidation in graphite, graphene will be laced with oxygen-containing groups and form a single-atomic-layered material known as Graphene oxide (GO). This process is easy to find at a low cost. Since it is dispersible in water and other solvents, it is easy to process. In addition, it is also used to create graphene. Graphene oxide is a lousy conductor. However, its properties could be improved by a unique process. Graphene oxide is usually in the form of powder, dispersed, or as a coating on the substrate ("Graphene-Info," 2017).

2.7 Zinc Oxide

In recent years, the interest of transition metal oxides nanomaterial and nano-sized semiconductor materials has been dramatically increased owing to their enormous desirable properties and applications in various areas such as chemistry, catalysts, biotechnology, photoelectron devices, environmental technology, sensors, information technology and highly functional and effective devices (Aneesh, Vanaja, & Jayaraj, 2007; Sangeetha, Rajeshwari, & Venckatesh, 2011; Z. L. Wang, 2004).

These nanomaterials have a wide bandgap between conduction and valence band and large surface area which result into higher surface energy, and consequently, it can show atom-like behaviours (Van Dijken, Meulenkamp, Vanmaekelbergh, & Meijerink, 2000). Therefore, a novel optical and electrical properties which are highly valuable in electro-optic applications can be obtained from these nanostructured materials. Moreover, metal nanoparticles are used in many biomedical applications to what it has from advantages such as self-cleaning, non-toxic and compatible with skin (Van Dijken et al., 2000).

The unique electrical and optical properties of nanoscale Zinc oxide (ZnO) have made it one of the best metal oxides to be used in broad applications such as many industrial areas, solar cells, cosmetic industries, gas sensors, optoelectronics and photo catalyst (Bose & Barua, 1999).

Furthermore, the broad chemistry and other favourable aspects of ZnO paved the way for many opportunities such as wet chemical etching, biocompatibility, radiation hardness and low power threshold for optical pumping (Sangeetha et al., 2011). These properties allow to ZnO to be an ideal material for various devices ranging from sensors through to ultra-violet laser diodes and nanotechnology-based devices like displays.

In fact, the optical properties of ZnO are greatly influenced by the lattice dynamics as well as the energy band structure. ZnO has direct band-gap of 3.4eV (Jagadish & Pearton, 2011) and exciton binding energy of 60 meV at room temperature (Bagnall et al., 1997). The lattice dynamics of ZnO is indicated in Figure 2.7. The figure illustrated a hexagonal lattice wurtzite (B4 type) structure of ZnO crystallised at a pressure and temperature of the ambient.

It can be clearly seen that the Zn ion is enclosed by a tetrahedron of O ions, and vice-versa. Therefore, the lattice can be characterised by two interconnecting sublattices of Zn^{2+} and O^{2-}. The polar symmetry which rises along the hexagonal axis due to the tetrahedral coordination is responsible for many of ZnO properties such as spontaneous polarisation and piezoelectricity. Additionally, this polarity is a crucial factor in etching, defect generation as well as crystal growth (Coleman & Jagadish, 2006).

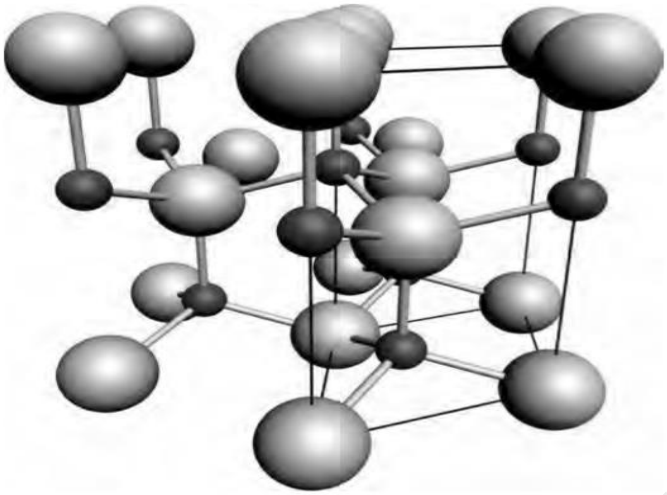

Figure 2.7: The hexagonal wurtzite structure of ZnO. O atoms are shown as large white spheres, whereas Zn atoms as smaller black spheres. One unit cell is outlined for clarity.(Coleman & Jagadish, 2006)

Usually, when the material has an ultrafast recovery time (~ps), wideband absorption, quite high damage threshold, appropriate modulation depth, low saturation intensity, simple fabrication process and economy, it is identified as an ideal saturable absorber for the fibre laser applications (Hasan et al., 2009). ZnO has a high third-order nonlinear coefficient, and it shows a recovery time as short as 1–5 ps when observed using time-resolved second harmonic generation (Johnson et al., 2004).

While the optical nonlinearities of ZnO have been investigated using the single-beam Z-scan method. The results of this investigation revealed that the nonlinear absorption of ZnO is due to the exciton energy level as well as two-photon resonance at the band edge while the optical nonlinearity is induced by the free carrier (Lin, Chen, Lin, & Hsieh, 2005).

Another investigation of the optical nonlinearity of ZnO using the same method showed a switchover from Reverse Saturable Absorption to Saturable Absorption which is an attractive characteristic for ultrafast optical switching applications; for instance, Q-switched and mode-locked fibre laser (Haripadmam, John, Philip, & Gopinath, 2014). Furthermore, ZnO has high sustainability to damage threshold, simple fabrication process and it is environment-friendly (Ahmad, Lee, et al., 2016; Jamdagni, Khatri, & Rana, 2016)

2.8 Summary

A saturable absorber is currently being in a top list because of a low cost and simple fabrication process. That is the reasons why for the past several years, various type of saturable absorber was being fabricated and undergoes research. The research is usually relating to the erbium-doped fibre laser to generate mode-locked and Q-switched pulsed. The main point of the research is to generate a high pulse of the laser. However, previous research had only been focused on the fabrication of a saturable absorber, while this thesis will be focused on the different technique to fabricate the saturable absorber and the effect of the film in the saturable absorber. Different technique to fabricate the SA can upgrade the wavelength for the better. The usage of a different film also might affect the generation of 1550nm wavelength. Therefore, both topics had been discussing in this thesis.

CHAPTER 3:

GRAPHENE OXIDE SATURABLE ABSORBER

3.1 Introduction

Q-switched fibre lasers have been widely studied to generate short laser pulses with high-energy for various applications, namely marking and machining, remote sensing, medicine, optical time domain reflectometry and laser ranging (Antipov et al., 2011; G. D. Spiers et al., 2011). There are two techniques to generate the lasers which are active or passive technique (M. Delgado-Pinar, Zalvidea, Diez, Perez-Millan, & Andres, 2006; Hisyam, Rusdi, Latiff, & Harun, 2016). The active Q-switching uses an optical modulator to periodically modulate the intra-cavity loss and turning the continuous wave (CW) laser into pulse trains. Therefore, the pulse repetition rate, as well as the pulse width, can be easily controlled. However, it is unfavourable to use an optical modulator as it is costly and has a complex operation. On the other hand, passive Q-switching has a unique advantage due to its simple structure in all-fibre designing. A saturable absorber (SA) is typically adopted in operations of all-fibre passive Q-switching. Different types of SAs have been proposed for Q-switching, for instance, semiconductor saturable absorber mirrors (SESAMs) (H. Y. Wang et al., 2012), carbon nanotubes (CNTs) (M. H. M. Ahmed et al., 2015; S. W. Harun et al., 2012) and graphene (Ahmad, Muhammad, Zulkifli, & Harun, 2013). SESAM has a modulation depth, which is usually less than 10% (Keller et al., 1996) and has a narrow wavelength tuning range (tens of nanometers). The CNTs and graphene are ideal SAs for Q-switching due to their low cost, broadband wavelength operation, as well as low saturation intensity (Bao et al., 2009).

A potential absorber to replace SESAMs for Q-switched or mode-locked lasers is graphene. However, graphene absorber is expensive since it is challenging to grow a high-quality graphene film. In addition, the efficiency for film fabrication by graphene aqueous solution is reduced because graphene cannot be dissolved in water. Traditionally, graphene oxide has served as a precursor for graphene due to its simple fabrication method and low cost (Boguslawski et al., 2015).

In this chapter, we demonstrate a Q-switched fibre laser with a new graphene oxide material as SA. The SA device is fabricated by embedding a graphene oxide material, which was obtained through chemical oxidation of graphite into two types of polymer which is PVA and PMMA film. Due to the unselective absorption of graphene absorber, it can be applied in a broad wavelength range. Stable and high power Q-switching pulses were achieved by incorporating a small piece of the film in an Erbium-doped fibre laser (EDFL) cavity.

3.2 Preparation of Graphene Oxide Saturable Absorber

3.2.1 Fabrication of Graphene Oxide Solution.

Graphene Oxide (GO) are fabricated by using Chemical oxidation of graphite was used to fabricate the graphene oxide (GO). Figure 3.1 summarises the fabrication process of GO solution. At first, 320 mL sulfuric acid (H_2SO_4), 80 mL phosphoric acid (H_3PO_4), 18g graphite flakes, and 18g potassium permanganate ($KMnO_4$) were mixed using a magnetic stirrer.

Graphite will undergo a process of exfoliation, which is the breakdown of van der wall forces when it is mixed with a strong acid such as sulfuric acids and phosphoric acids. Combination of sulfuric acids and phosphoric acids are safer since it would not

produce toxic gas. This process required potassium permanganate to oxidise the graphite after the forces are a break. All the materials have been slowly added to avoid an incomplete oxidation process. The one-pot mixture was left for stirring for three days in order for the oxidation of graphite to take place.

The mixture changed its colour from dark purplish green to dark brown after three days. Hydrogen peroxide (H_2O_2) solution was then added in the mixture to remove all the excessive potassium permanganate ($KMnO_4$). As a result, removing the excessive $KMnO_4$, the oxidation process will be stopped, and the colour of the mixture will turn to bright yellow. This indicates a high oxidation level of graphite. The graphite oxide formed was washed three times with 1 M of hydrochloride (HCl) aqueous solution and repeatedly with deionised water until a pH of 4–5 was achieved.

The washing process was carried out by simple decantation of supernatant via a centrifugation technique. To conduct a centrifuge technique, deionised water and graphite oxide are injected in the same tube. The tube then is closed and placed in the centrifuge device under the centrifugation force of 10,000 g. More Graphite Oxide mixture compares to its original volume are produced due to the distorted of the lid of the tube by the force from the centrifuge. At the same time, Graphene Oxide with a high density will be started to be formed at the outer edge due to the centrifuge force, while leaving the excessed waste with the deionised water on the top of the tube. After a while, the centrifuge force will slow down, and the tube lids reshape to the origin.

Throughout the washing process using deionised (DI) water, the graphite oxide undergoes exfoliation, which leads to the thickening of the graphene solution, forming a GO gel. To achieve a graphene oxide solution, the GO gel was then mixed with the DI water. Then the mixture was stirred for 2 hours to get a homogenous GO solution.

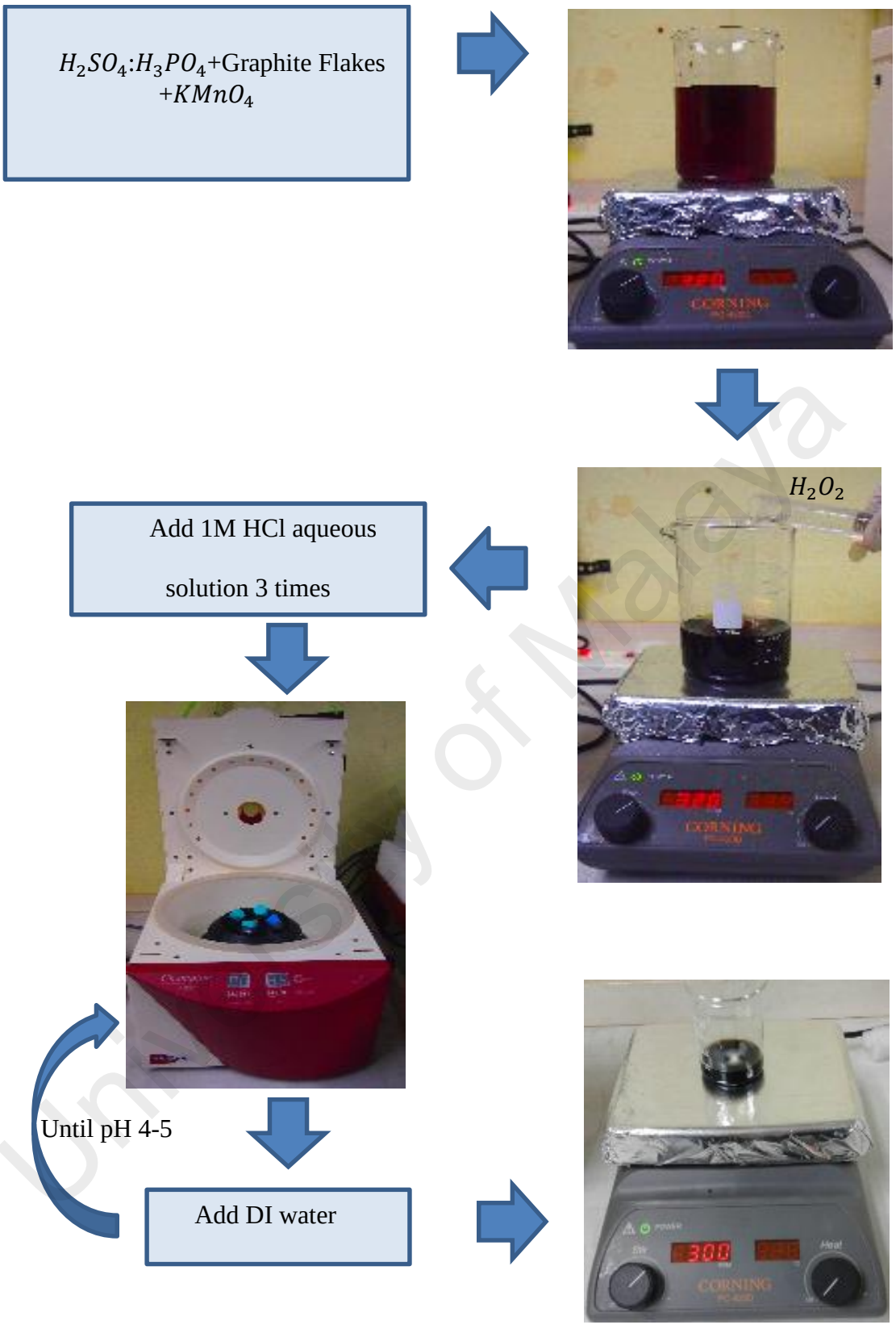

Figure 3.1: Step by step procedures for the fabrication of GO solution

3.2.2 Preparation of GO PMMA

The GO was embedded into two types of polymer in this study; Poly(vinyl alcohol) (PVA) polymer and Poly(Methyl Methacrylate) (PMMA) to compare their performance for Q-switching pulses generation. To prepare the GO-based PMMA polymer, 2g of polymethylmethacrylate (PMMA) powder was dissolved in 60 ml of acetone and heated at 30°C with slow stirring until the PMMA completely dissolved and form a PMMA solution. Then, the graphene oxide solution was mixed together with PMMA, followed by slow stirring for the duration of 2 hours. The mixture solution was then poured into a petri dish and being left to dry for 2 days in ambient. The film was peeled slowly after it has dried.

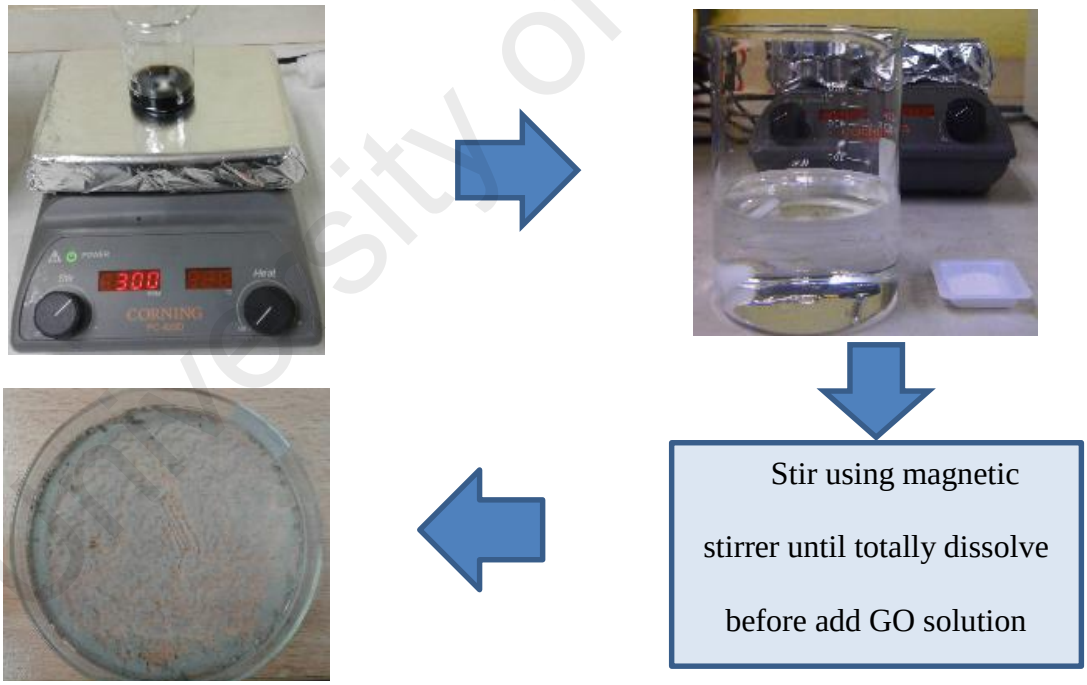

Figure 3.2: Fabrication of GO PMMA thin film

3.2.3 Preparation of GO PVA

The GO-based PVA thin film is summarised in Figure 3.3. The process starts by preparing the PVA solution. Firstly, PVA powder is dissolved [40000 MW, Sigma Aldrich] into 80 ml of Deionised (DI) water in a beaker and then it was stirred by using magnetic stirrer at a temperature of 145 °C until the mixture completely dissolves. After that, the prepared PVA solution was mixed with the homogenous GO solution and being stirred slowly for two hours. The mixture solution was poured into a petri dish and subsequently left to dry at room temperature. After two days, the thin film can be peeled slowly from the petri dish.

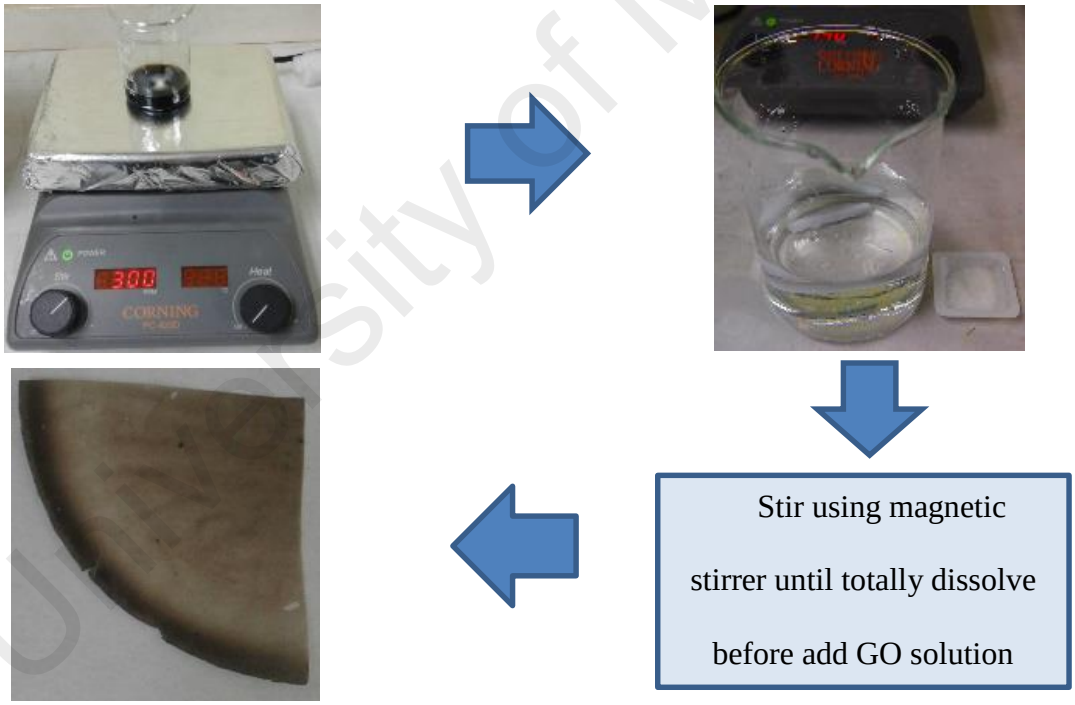

Figure 3.3: Fabrication of GO PVA thin film

3.3 Experimental setup for the Q-Switched EDFL using GO SA

The experimental setup of the proposed Graphene Oxide based Q-switched EDFL is schematically shown in Figure 3.4. The laser cavity consists of a 2.8m long erbium-doped fibre (EDF) as the gain medium, an isolator, a wavelength division multiplexer (WDM), the fabricated GO PMMA or GO PVA film-based SA device and an 80/20 output coupler in a ring configuration. A fibre-coupled laser diode which has a centre wavelength of 980 nm was used as the pump source. It is launched into the EDF via WDM. The EDF used has an Erbium ion absorption of 23 dB/m at 980 nm with a core and cladding diameters of 4 µm and 125 µm respectively as well as a numerical aperture (NA) of 0.16. A polarization independent isolator was used to ensure unidirectional propagation of the oscillating laser in the ring laser cavity. An 80:20 output coupler was used to couple out the laser signal, where it keeps 80% of the light oscillating, in the ring cavity for both spectral and temporal diagnostics and 20 % as the output. An optical spectrum analyzer (OSA) with a spectral resolution of 0.02 nm was used to evaluate the spectral characteristic while a 500 MHz oscilloscope and a 7.8 GHz radio-frequency spectrum analyzer with a 1.2 GHz photodetector were used to measure its temporal characteristics.

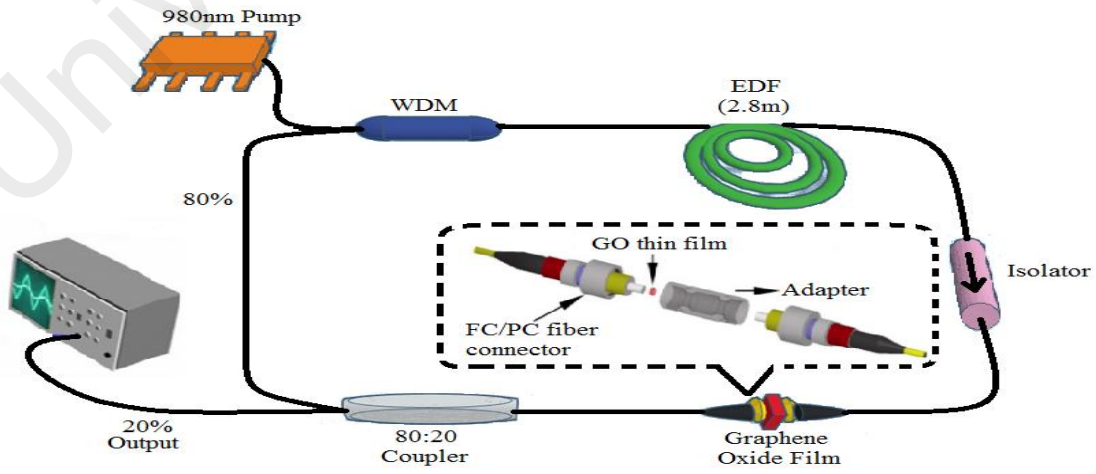

Figure 3.4: Configuration of the Q-switched EDFL employing a GO film as a Q-switcher

3.4 Q-switching performance with Graphene Oxide PMMA SA.

3.4.1 GO PMMA Thin Film Characteristic

The quality of GO PMMA film was verified by observing its Raman Spectrum. In the experiment, an Argon ion laser which operates at 514 nm was used as a light source. The laser was radiated on the film for a duration of 10 ms with 50 mW exposure power. Figure 3.5 presents the Raman spectrum, where it can be seen that the D peak of GO is located at 1359 cm^{-1} while the G peak is located at around 1600 cm^{-1}. The defect-induced breathing mode of sp^2 rings caused the D band while the first order scattering of the E_{2g} phonon of sp^2 carbon atoms caused the G band to occur (Ferrari & Robertson, 2000). It can be seen in Figure 3.5, that this G band of the GO is located at a higher frequency compared to graphite 1580 cm^{-1} and this corresponds to the finding reported by (Kudin et al., 2008). The (I_D/I_G) intensity ratio which is calculated by inversely proportional to the average size of the sp^2 clusters to measure the disorder degree give a GO value ratio of 0.85 (Sobon et al., 2012). In order, to determine the insertion loss, the fabricated GO film is sandwiched between two fibre ferrules inside a physical contact ferrule connector to form an all-fibre SA device. In order to reduce the insertion loss, an index-matching gel is deposited between the fibre ferrules. The insertion loss of the GO-based SA device is measured during the experiment, and it is around 3 dB at 1550 nm. For the Q-switching experiment, the SA device will be incorporated in an EDFL cavity.

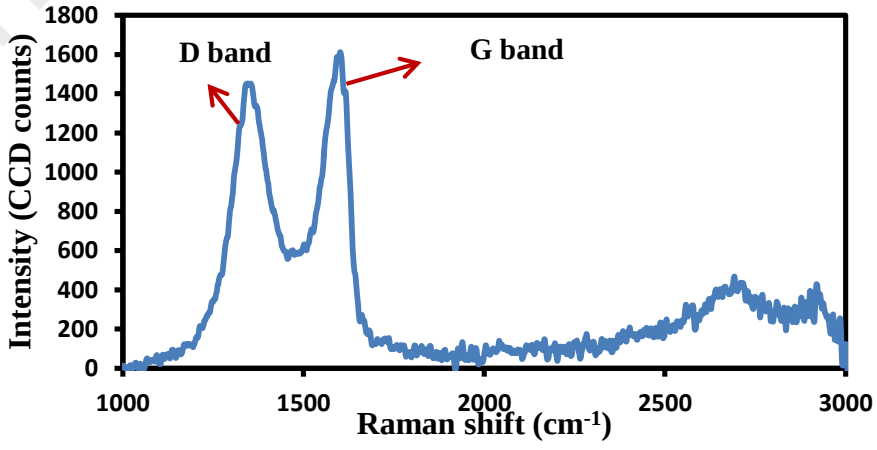

Figure. 3.5: Raman spectrum of the GO PMMA film

3.4.2 Result and Discussion

Stable and self-starting Q-switching operation was achieved by increasing the pump power to more than 11.8 mW. It should be noted that below the threshold pump power, there was no lasing. Such a low threshold power for Q-switching operation was most probably due to the small intra-cavity loss of the GO PMMA SA. Within the pump power of 11.8 to 83.0 mW, a stable pulse train with an increasing repetition rate was observed and this indicates a typical characteristic of a Q-switched laser. Figure 3.6 (a) presents the EDFL output spectrum at a pump power of 83.0 mW. From the figure, it can be seen that the laser operated at the centre wavelength of around 1531.6 nm. Due to the Self-Phase Modulation (SPM) effect in the laser cavity, spectral broadening was seen in the spectrum.

Figure 3.6 (b) illustrates the typical oscilloscope trace of the Q-switcher pulse train at a pump power of 83.0mW. It can be seen that the peak-to-peak duration is 14.55 μs, which is equivalent to the repetition rate of 68.7 kHz. Besides that, a stable Q-switched pulse output can be observed and there were no amplitude modulations in the pulse train. This shows that during the Q-switching operation, there was no self-mode locked locking effect.

A single envelope of the Q-switching pulse is shown in the inset figure of Figure 3.6 (c). It has a pulse width of approximately 6.12 μs with a nearly symmetrical shape. The film was removed from the ring cavity to verify that the passive Q-switching was attributed to the GO PMMA SA. In this case, even when the pump power was adjusted over a wider range, there were no Q-switched pulses observed on the oscilloscope. Hence, this proved that the GO film was responsible for the passively Q-switched operation of the laser.

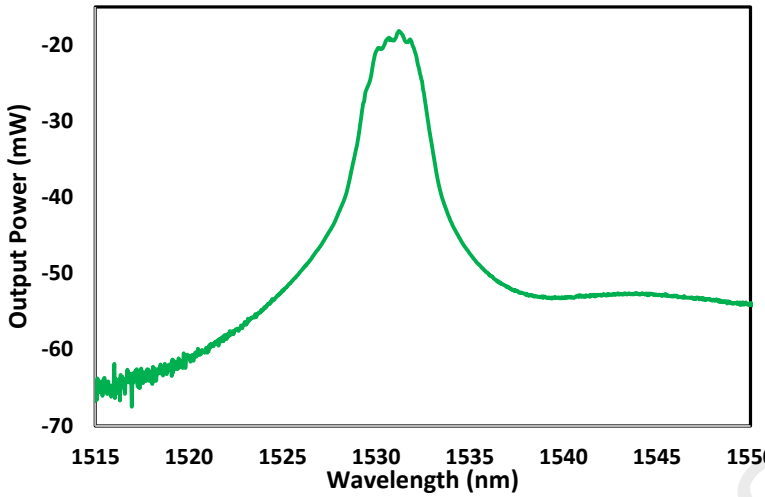

(a)

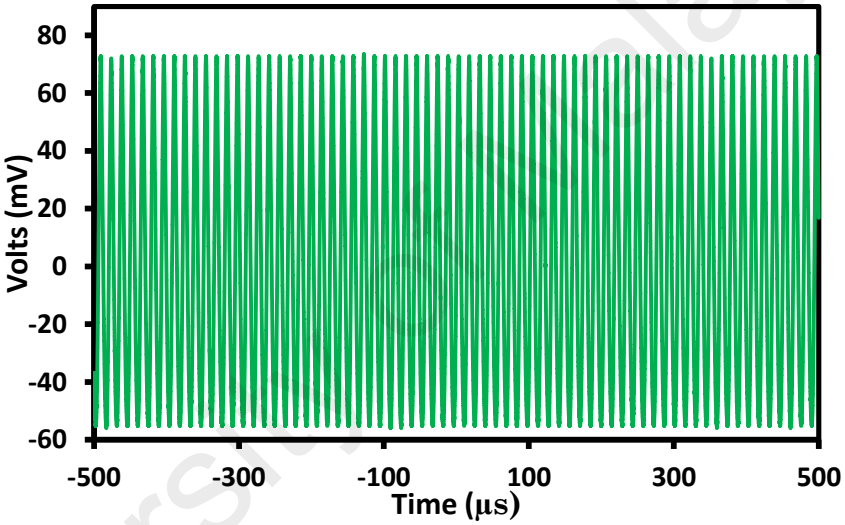

(b)

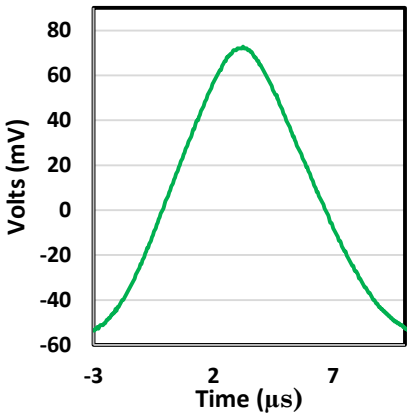

(c)

Figure 3.6: Pulse characteristic at the pump power of 83.0mW (a) Pulse wavelength (b) Typical pulse train (c) Single envelop pulse

Figure 3.7 demonstrates the relationship between the pulse repetition rate and pulse width with pump power. When the pump power rises from 11.8 mW to 83.0 mW, the repetition rate rises almost linearly from 21.5 kHz to 68.7 kHz with the pump power rate of ~0.64 kHz/mW. This is because as the pump power increases, more gain is given to saturate the SA and hence causes the repetition rate to increase. On the other hand, pulse duration reduces from 20.44 µs to 6.12 µs as the pump power rises. We observe that the pulse duration exponentially drops at a lower pump power (< 30 mW), and a smaller change of pulse width start at the higher pump power (>30 mW). Pulse width decreases linearly while the repetition rate rises. As the pump power is increased, more photons circulate inside the laser cavity, and hence the SA is becoming saturated. The minimum attainable pulse duration is 6.12 µs, and it is believed to be related to the modulation depth of the SA. Shortening the cavity length and improving the modulation depth of the SA could further reduce the pulse duration.

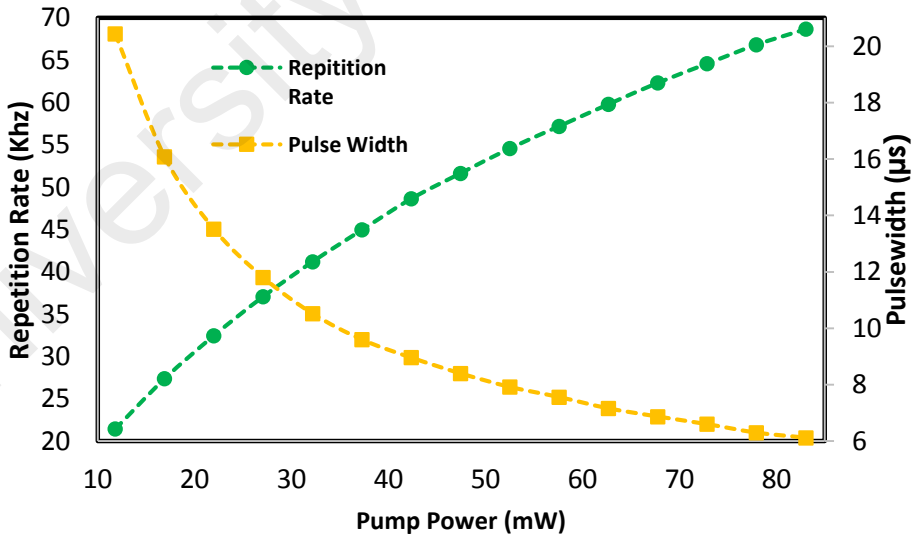

Figure 3.7: Pulse width and repetition rate versus incident pump powers of GO PMMA

Figure 3.8 demonstrates the relationship between the average output power and pulse energy with pump power for the proposed Q-switched EDFL. When the pump power rises, the average output power also rises, which leads to an increased in pulse energy. It can be seen that the output power is increased linearly from 1.00 mW to 9.96 mW with a slope efficiency of 12.52% by tuning the pump power from 11.80 to 83.00 mW. As the pump power rises from 11.8 mW to 83.0 mW, the pulse energy increased from 46.6 nJ to 145.0 nJ. The increment of pump power gives rise to the average output power and shortening the pulse width and therefore, in the Q-switching process, the higher pulse energy is extracted.

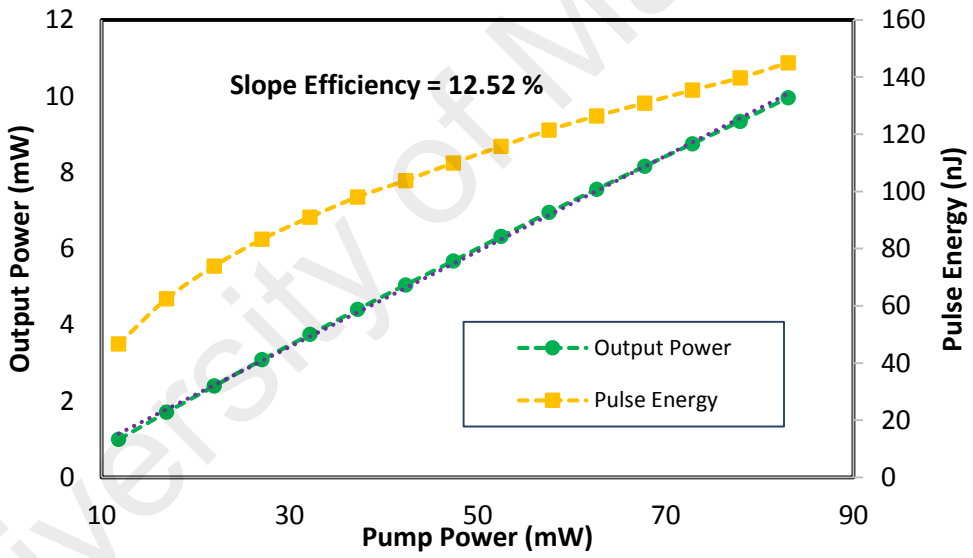

Figure 3.8: Average output power and pulse energy versus incident pump power of GO PMMA

Q-switched pulsed stability can be investigated from the radio frequency (RF) spectrum as shown in Figure 3.9. The RF spectrum illustrated a high signal to noise ratio (SNR) of 62.6 dB with a fundamental frequency of 68.7 kHz. The SNR indicates good pulse train stability as comparable to Q-switched fibre lasers with CNT and graphene (Ahmad et al., 2013; M. H. M. Ahmed et al., 2015; S. W. Harun et al., 2012).

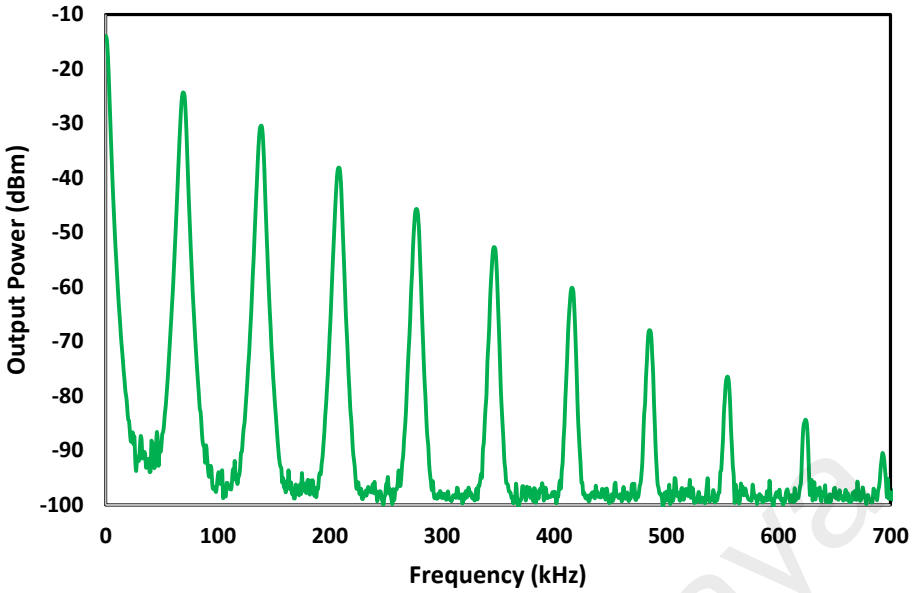

Figure 3.9: RF spectrum of the Q-switching pulse at a pump power of 83.0 mW in GO PMMA

There are no significant changes observed in any of the output parameters of the proposed laser after two hours of operation or the next following two days, and hence the proposed laser is highly stable. As the pump power greater than 83.0 mW, the Q-switched pulses became unstable and switched to CW mode, as reported previously (Ahmad et al., 2013; M. H. M. Ahmed et al., 2015; S. Harun et al., 2012). The unstable Q-switched might be caused by the over-saturation of the GO film at high incident intensity. In this situation, under the high optical intensity, the two-photon absorption (TPA) process in the GO layer has been excited. Therefore, as the pump power is continuous increases, the absorption coefficient is also increased. Hence, the Q-switched operation could not be maintained. As the pump power is reduced from 200 mW, stable Q-switched operation could be seen again at the pump power of 83.0 mW and below, which indicates that at relatively high power, the sample was not damaged. In the lasers, no thermal damage is observed in the GO film sample and during the laser operation up to 83.0 mW, the output power was stable.

3.5 Q-switching performance with Graphene Oxide PVA SA

3.5.1 GO PVA Thin Film Characteristic

Figure. 3.10 (a) illustrates the Raman spectrum of the GO PVA film, which was excited by an Argon ion laser operating at 514 nm. Two prominent peaks of GO can seemed from the spectrum at 1357 cm^{-1} and 1606 cm^{-1}, which are assigned to D and G bands, respectively. The D band corresponds to the structural imperfections due to the attachment of hydroxyl and epoxide groups on the carbon basal plane while the G band is obtained due to ordered sp^2 bonded carbon. It is worthy of mentioning that the 2D band was hardly observed in the spectrum. It was normally observed at 2700 cm^{-1} for graphene material. This indicates that there was no reduced graphene on the GO film.

Figure 3.10 (b) presents the image of the film, which has a thickness of approximately 50 µm. Other characteristics of the GO SA, which can potentially affect the performance of the fibre laser, were also investigated. For instance, the morphological property of the film was investigated with field emission scanning electron microscope (FESEM), and the image is shown in illustrated in Figure 3.10(c). We can see there are no obvious air holes or bubbles in the GO-PVA polymer film, which indicates the excellent uniformity of the SA. The present of > 1µm aggregates or voids in the composite SA may lead to non-saturable scattering losses.

The fabricated GO PVA film was also cut into a small piece and is being attached into an FC/PC fibre ferrule. After placed an index matching gel onto the fibre end, the ferrule was matched with another fresh ferrule through a connector to construct an all-fibre SA device. The insertion loss of GO PVA based SA device was also measured during the experiment. It has almost similar loss with the previous GO PMMA based device, which was around 3 dB at 1550 nm.

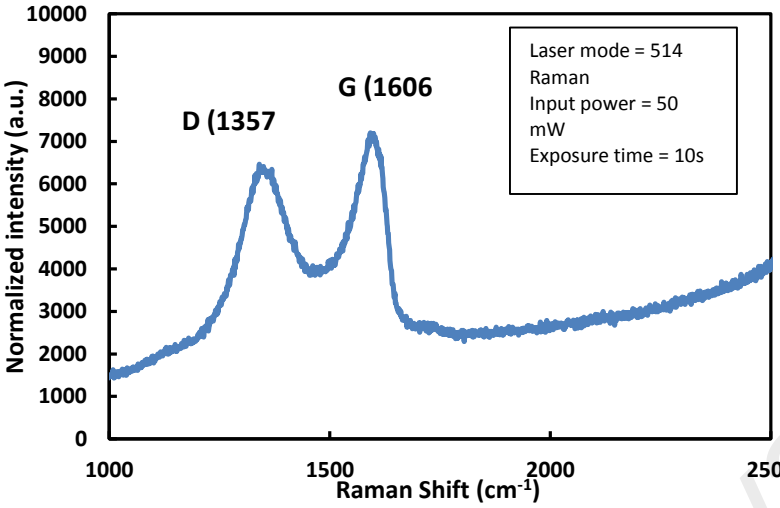

(a)

(b)

(c)

Figure 3.10: Characteristic of GO PVA (a) Raman spectrum (b) FESEM image (c) Actual image

3.5.2 Result and Discussion

With GO PVA film-based SA device, the EDFL obtained a stable and self-starting Q-switching operation at a pump power of 16.88mW. Below the threshold pump power, no laser is detected. As compared to the previous PMMA film, the threshold is slightly higher. This is most probably caused by the transmission loss, which is slightly greater with the PVA. It could be seen that as the pump power increases from 16.88mW to 72.85mW, a stable pulse train could be observed with an increasing value of repetition rate. This criterion follows the typical Q-switched laser characteristic. As the pump power has risen to 72.85mW, the output spectrum of the EDFL cavity can be observed where the laser wavelength operates at a centre of 1560.5 nm as shown in Figure 3.11 (a). Compared to the previous result (GO PMMA), the spectral broadening is not obvious in the laser output. This is most probably due to the PVA film has a lower nonlinearity compared to the GO PMMA one.

The typical pulses train of the Q-switched laser is also investigated using an oscilloscope as demonstrated in Figure 3.11 (b). This figure illustrates the pulses train at a pump power of 72.85mW, which indicates the pulses period of 12.24μs and this corresponds to the repetition rate of 81.7 kHz. It can be seen that the pulses train in the Q-switched output is stable without any amplitude modulations in the pulse. This proves that during the Q-switching operation, no self-mode locking effect is detected. The pulse has an almost symmetry shape with a pulse width of approximately 5.67 μs as presented in the inset of Figure 3.11 (c). Fibre ferrule filled with GO PVA film was replaced with a common clean ferrule to verify that the passive Q-switching was attributed to the GO-based SA. In this case, even when the pump power was adjusted over a wider range, no Q-switched pulses were observed on the oscilloscope. With SA, the stable Q-switching operation was maintained within the pump power from 16.88mW to 72.85mW.

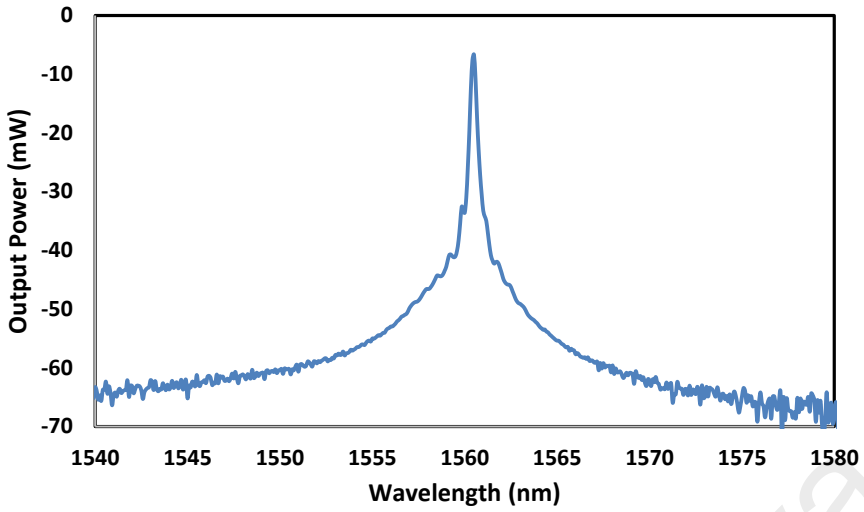

(a)

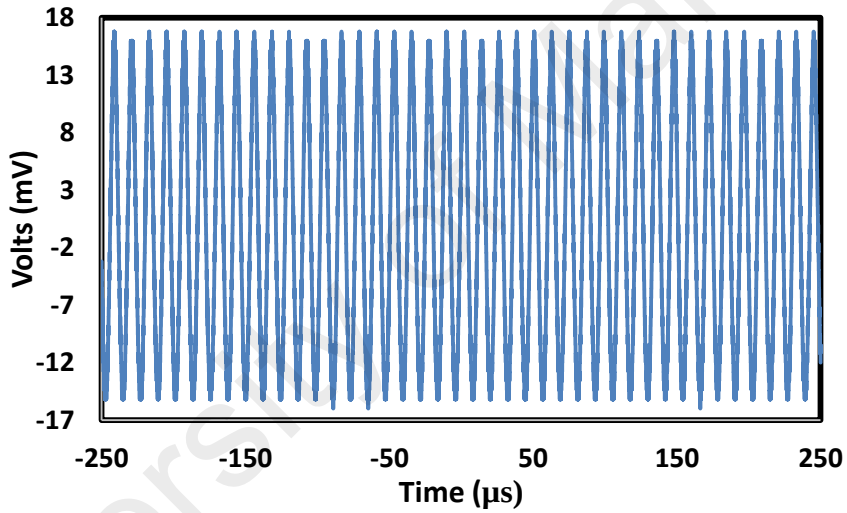

(b)

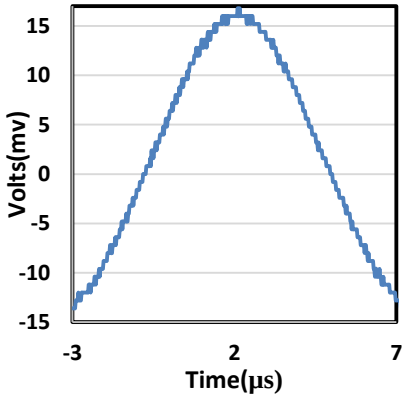

(c)

Figure 3.11: Pulse characteristic at the pump power of 72.85mW (a) Pulse wavelength (b) Typical pulse train (c) Single envelop pulse

Figure 3.12 demonstrates the relationship between the pulse width and pulse repetition rate with pump power. As illustrated in the Figure3.12, the rising of the pump power from 16.88 mW to 72.85 mW has resulted in a rising of repetition rate from 32.45 kHz to 81.7 kHz. The repetition rate has increased almost linear manner with a pump power rate of 0.87 kHz/mW. This shows that by increasing the pump power, the repetition rate of the Q-switched pulses train can be tuned. The increasing of the pump power also will provide more gain to saturate the GO PVA SA, hence, causes the repetition rate to increase.

The relationship between the pulse width and pump power are opposite to the repetition rate. As pump power is increased, the pulse width duration reduces from 14.28 μs to 5.67 μs. Pulsed width decreases exponentially as the pump power rises from 16.88mW to 29.00 mW. The drop is rapid since the GO PVA is still not saturated and thus able to generate more gain. As the pump power rises from 30.00 mW to 72.85 mW, pulse width starts to drop linearly because the SA become saturated as the pump power continuously rises. The pulse will change to continuous wave (CW) mode at a pump power more than 72.85mW.

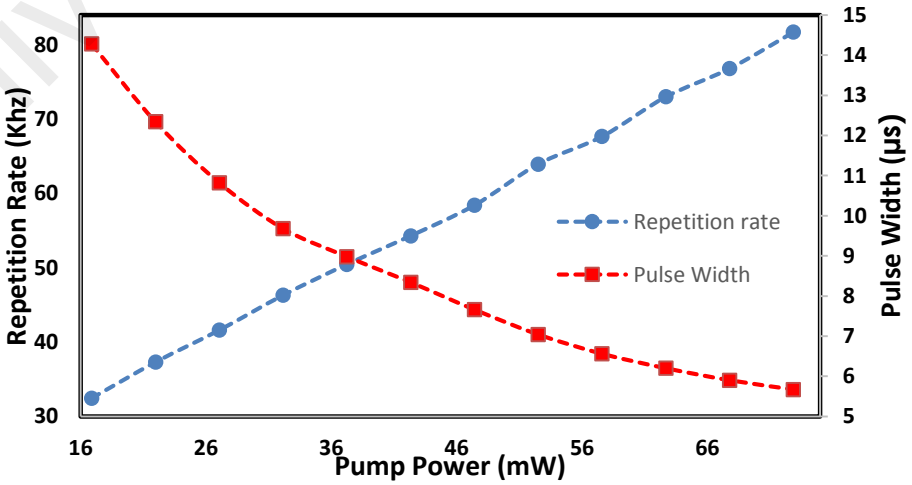

Figure 3.12: Pulse width and repetition rate versus incident pump power for the EDFL configured with GO PVA film-based SA

The relationship between pulse energy and average output power with pump power in the proposed Q-switched EDFL are demonstrated in Figure 3.13. It is demonstrated in the graph that pulse energy and output power are increase with the increase of pump power. For instance, as the pump power is adjusted from 16.88mW to 72.85mW, the output power risen linearly from 1.59 mW to 8.93mW. This output power curve also shows the slope efficiency obtained for the Q-switched EDFL is about 13.15%.

In contrast, the pulse energy increases from 48.99 nJ to 109.30 nJ when the pump power is increased from 16.88 mW to 72.85 mW. In general, increasing pump power improves the gain, which in turn increases the output power. Higher output power decreases the pulse width, which results in the generation of higher pulse energy to be extracted in the Q-switching process. Compared to the GO PMMA based laser, the maximum achievable pump power is lower in this laser.

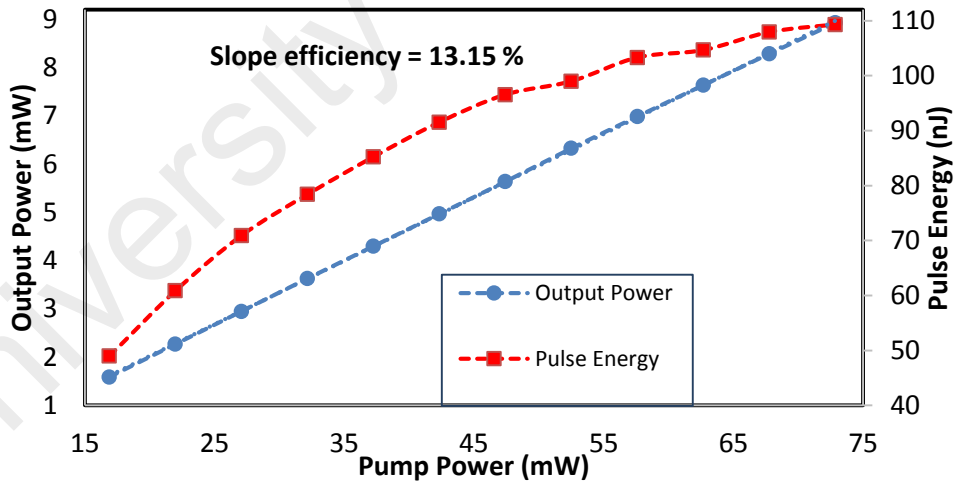

Figure 3.13: Average output powers and pulse energies versus incident pump power for the GO PVA based Q-switched EDFL.

Figure 3.14 illustrates the radio-frequency (RF) spectrum of the laser at the pump power of 72.85mW. Radio-frequency (RF) spectrum can be used to determine the

stability of the Q-switched pulses. The fundamental frequency in the RF spectrum is obtained at 81.7 kHz. The SNR for the fundamental frequency is about 61.76 dB, which indicates that the laser has excellent stability.

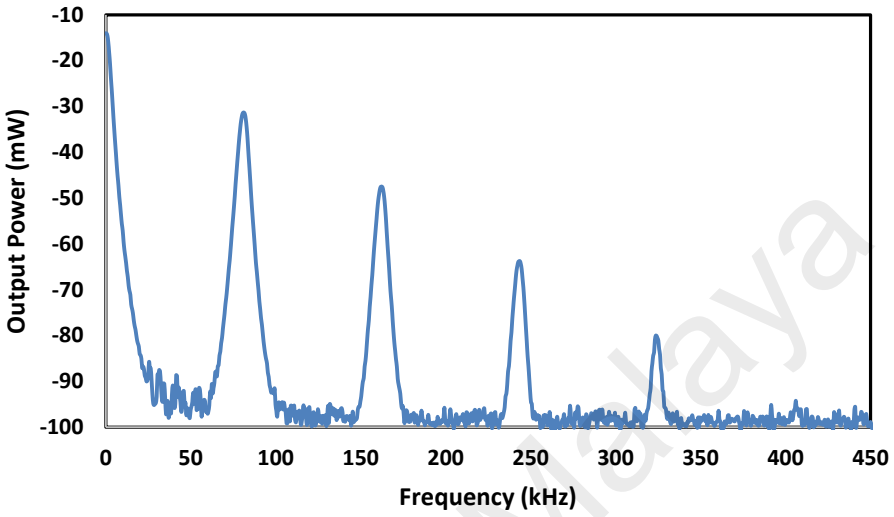

Figure 3.14: RF spectrum of the Q-switching pulses at the pump power of 72.85mW with the incorporation of GO PVA based SA

To further examine the stability of the Q-switched laser, it was left to run for about two days. It was observed that the output pulses and highly stable without significant changes. The Q-switching output pulsed becomes unstable and switches to CW mode when the pump power rises above 72.85 mW. However, as the pump power decreased back within the operating region from 16.88mW to 72.85mW, the Q-switching pulses were generated. This shows that the SA is not broken even it is imposed with relatively high power.

Besides that, during the laser operation, there is no thermal damage observed in the GO film sample. This verifies that the SA is over saturated after the pump power reaches 72.85 and causes the Q-switched laser becomes unstable if the pump power further increases. In other words, under the higher optical intensity, two-photon

absorption (TPA) process in the GO layer has been excited, and this results in the rising of the absorption coefficient as the pump power is increased. Hence, the Q-switched operation could not be maintained.

Since the maximum pump power is only about 200mW, it is difficult to measure the damage threshold accurately. From the observation, it can be figured out that by optimising the cavity by decreasing the cavity length and cavity losses, a better Q-switched pulse can be generated. Optimising the cavity structure or using an excellent grade of graphite during fabrication of GO can also help in generating a better Q-switched pulse.

3.6 Summary

Passive Q-switched EDFLs have been successfully demonstrated using the newly developed GO PMMA and GO PVA film based SAs. The SA device was fabricated by embedding a GO material, which was obtained through chemical oxidation of graphite into both polymers.

By incorporating GO PMMA SA into an EDFL cavity, stable Q-switched pulses were generated to operate at 1531.6 nm when the pump power was changed within a range of 11.8 to 83.0 mW. As the pump power increases within this power range, the repetition rate could be increased from 21.5 kHz to 68.7 kHz, and pulse duration could be reduced from 20.44 μs to 6.12 μs. The pulse energy was 145 nJ at the pump power of 83.0 mW.

On the other hand, GO PVA film-based SA device can also be used to generate a stable Q-switching pulse train that operating at a longer wavelength of 1560.5 nm. With the GO PVA SA, the Q-switched was realised within a pump power range between

16.88mW to 72.85mW. As the pump power gradually increased, the repetition rate has risen from 32.45 kHz to 81.7 kHz while the pulse duration or pulse width drops from 14.28 μs to 5.67 μs. At the maximum pump, the highest repetition rate and single pulse energy of 81.7 kHz and 109.30 nJ were achieved.

These results show that GO PMMA film has a better performance compared to the PVA film in terms of the pulse energy and operating pump power range. It is believed that both GO-based SA devices have a great potential for Q-switching and even mode-locking pulses generation in 1.5-micron region.

CHAPTER 4:

ZINC OXIDE SATURABLE ABSORBER

4.1 Introduction

Over a past one quarter century, transition metal oxide like titanium dioxide (TiO_2), zinc oxide (ZnO) and cobalt oxide (Co_3O_4) have being commercially investigate as one of an alternative for a nonlinear optical materials because of their great characteristic such as large optical non linearity, good thermal and chemical stability with an addition of mechanical strength. ZnO has a direct band-gap of 3.4eV (Jagadish & Pearton, 2011) and high energy of 60 meV (Jagadish & Pearton, 2011; Reynolds et al., 1996) at room temperature, making it a strong potential candidate for developing pulsed output. Furthermore, ZnO has additional favourable properties which make it highly suited towards optical applications, including biocompatibility, radiation hardness, low power threshold for optical pumping and wet chemical etching (Janotti & Van de Walle, 2009). These characteristics make ZnO a highly valuable candidate for emerging electro-optical applications (Janotti & Van de Walle, 2009) and become a highly viable candidate as a material for saturable absorption. In this chapter, two Q-switched Erbium-doped fibre lasers (EDFLs) are proposed and demonstrated using a ZnO powder as a base material for a saturable absorber. At first, the SA is fabricated by embedding a prepared ZnO powder into Poly(methyl methacrylate) (PMMA) film. By incorporating a small piece of the film in a laser cavity, the proposed laser generates a stable Q-switched pulses train at 1559.3 nm with repetition rate rises from 24.85 to 85.91 kHz whereas the pulse width reduces from 17.88 to 4.66 μs as the pump power was increased from 12 to 98.49 mW. By replacing the polymer material from PMMA to poly(vinyl alcohol) (PVA), the EDFL produces a stable Q-switched pulses train with a higher pulses energy

4.2 Preparation of Zinc Oxide based Saturable Absorbers

4.2.1 Preparation of Zinc Oxide powder

At first, the ZnO powder was prepared to fabricate the ZnO based SA. In the process, 10 mM of Zinc Nitrate Hexahydrate [Zn(NO3)2·6H2O, Ajax Finechem Pty Ltd] and Hexamethylenetetramine [(CH2)N4, Sigma-Aldrich] was dissolved in 600 ml of DI water under stirring for 15 minutes. Then, the 100 ml of the solution was poured into a separate beaker and placed in the oven for 5 hours. After 5 hours, white precipitates were formed due to the existence of ZnO element. The precipitates were collected and left to dry in ambient conditions for 2 days. Figure 4.1 shows a step by step procedure to prepare the ZnO solution. The preparation of PMMA and PVA polymers solution and fabrication to the thin film will be discussed in section 4.2.2 and 4.2.3.

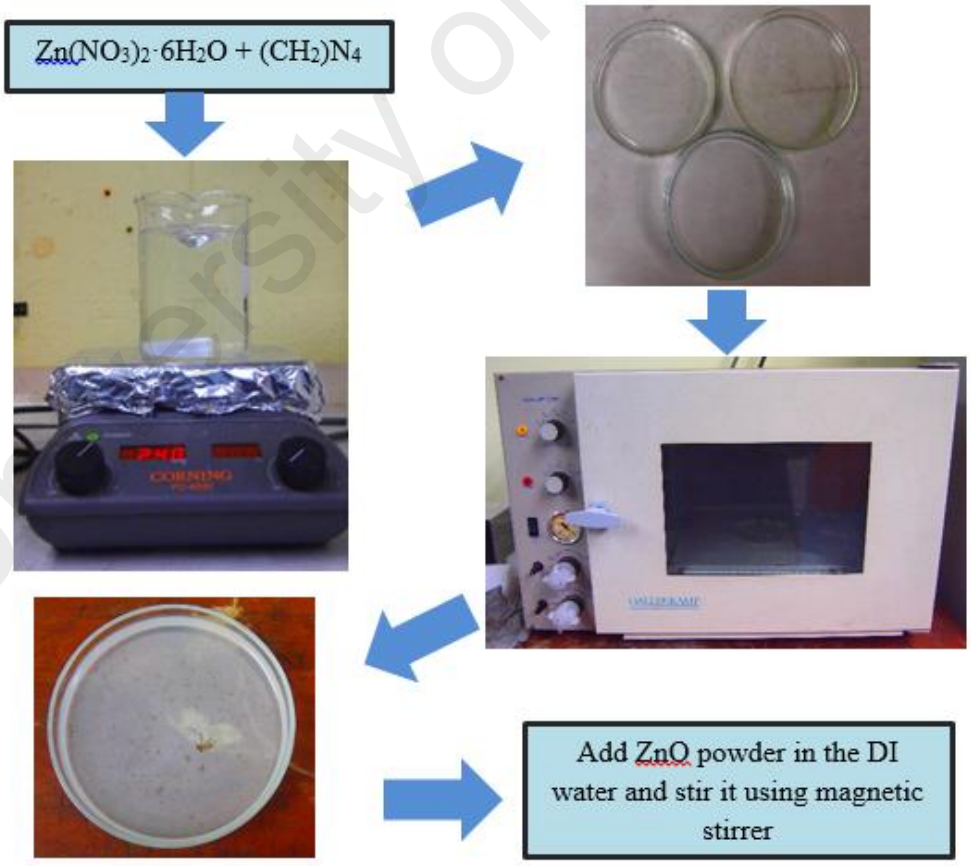

Figure 4.1: Preparation of ZnO powder

4.2.2 Preparation of Zinc Oxide PMMA thin film

To prepare the polymer solution, 2g of PMMA was dissolved in 60 ml of acetone and heated at 30°C with slow stirring until the PMMA completely dissolved. After that, 0.030g of the ZnO powder was mixed with a PMMA solution with the assistance of slow stirring for two hours. Then, the mixture solution was poured into the petri dish and left dry in ambient for two days. After dry, the film was slowly peeled out to obtain a ZnO PMMA film.

Figure 4.2: Fabricate ZnO PMMA thin film

4.2.3 Preparation of Zinc Oxide PVA thin film

To fabricate the ZnO PVA thin film, the PVA solution was prepared by dissolving PVA powder [40000 MW, Sigma Aldrich] into 80 ml of DI water and stirred at 145ºC until it completely dissolves. Then, the ZnO powder was dissolved in 10 ml of DI water and centrifuged for 10 minutes to form ZnO solution. Then, the solution was mix with PVA solution and followed by slow stirring for two hours. The mixture solution was poured into the petri dish and left dry in room temperature. After two days, the ZnO PVA film was slowly peeled from the petri dish.

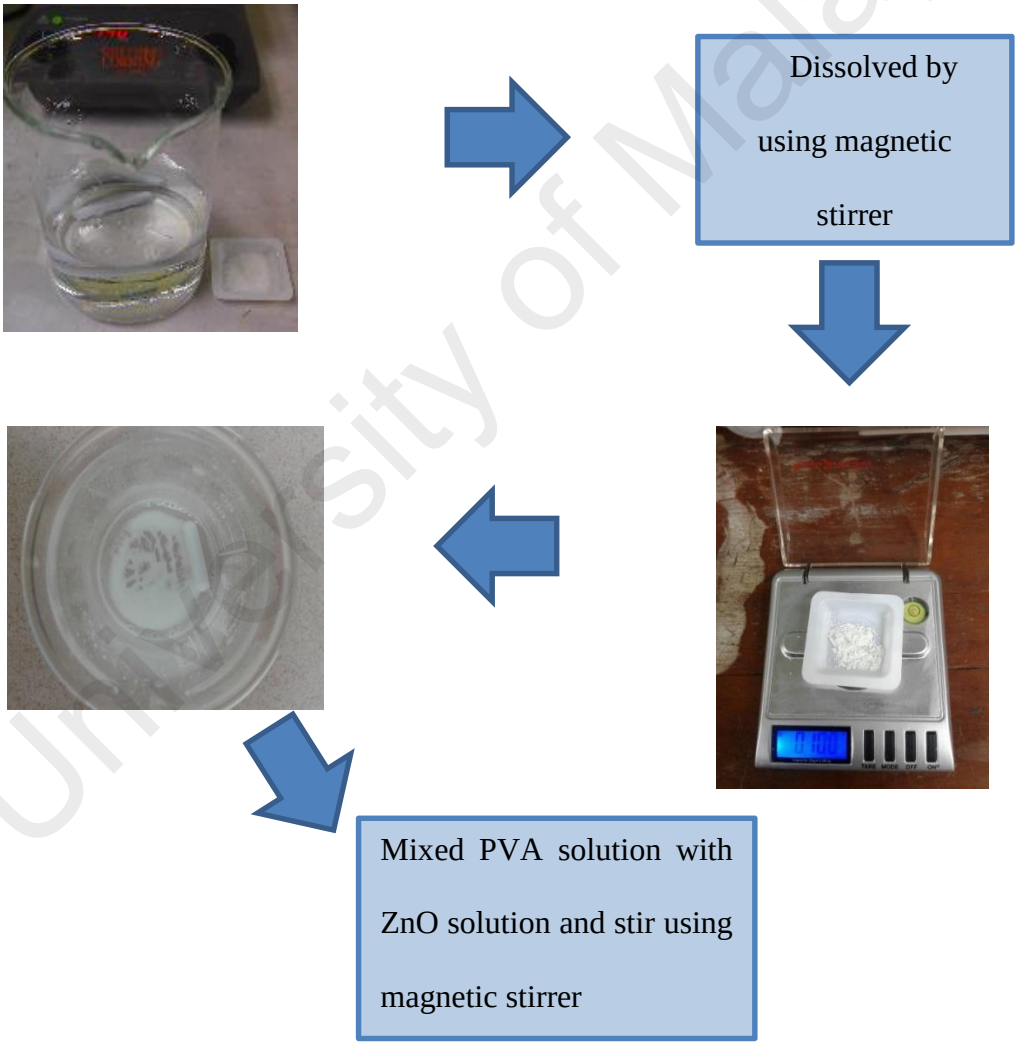

Figure 4.3: Fabricate ZnO PVA thin film

4.3 Laser Configuration

Figure 4.4 demonstrates a schematic layout of an incorporating EDFL cavity with ZnO based SA to generate the passive Q-switched pulse. By using 980/1550 nm wavelength division multiplexer (WDM), a 980 nm laser diode is pump into 2.8 m long Erbium-doped fibre (EDF). The EDF has a 4 µm diameter of the core and 125 µm diameter of the cladding with the amount of 0.16 numerical aperture (NA), where the Erbium ion is able to absorb 23 dB/m at 980 nm. To minimise the possibility of the light to reflect multidirectional while being transmitted in the cavity, the used of polarisation independent isolator are necessary. ZnO film that being fabricate earlier was integrated into the ring cavity to act as a passive Q-switcher. The laser signal that passes through the ZnO film is coupled out using 80:20 output coupler. Eighty percent (80%) of the light remains in the ring cavity and continue oscillating for both spectral and temporal diagnostics while 20% of the light is used for output measurement. The spectral characteristic was measured by using a 0.02nm spectral resolution of the optical spectrum analyser (OSA), while the temporal characteristics were measured using a 500 MHz oscilloscope and a 7.8 GHz radio-frequency (RF) spectrum analyser via a 1.2 GHz photodetector.

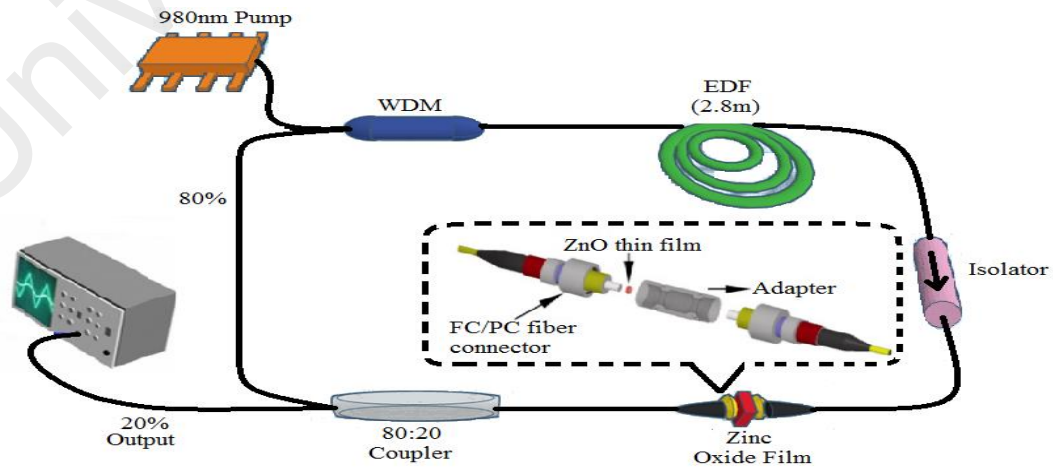

Figure 4.4: Configuration of the Q-switched EDFL setup employing ZnO film as a Q-switcher

4.4 Q-switching performance with ZnO PMMA film

4.4.1 Result and Discussion

Passively Q-switching from the constructed EDFL cavity is self-begins at a pump power of 12 mW. Compared with the reported works (Fan et al., 2014), the threshold power of this laser is relatively low, which is attributed to the larger third-order optical nonlinearities induced by the ZnO based SA. The Q-switching operation was maintained up to the pump power of 98.49 mW. Figure 4.5(a) demonstrated an output spectrum of the Q-switching laser at a pump power of 98.49 mW. This figure illustrates that the 3 dB bandwidth of the optical spectrum was 2.8 nm at the centre wavelength of 1559.3 nm. It is relatively broad due to the self-phase modulation effect that being induced from ZnO SA film in the ring cavity.

The Q-switched pulse train was also measured using an oscilloscope as shown in Figure 4.5(b) at the pump power of 98.49 mW. Q-switched output power pulse at this pump power has a peak to peak duration of 11.64 µs, which is equivalent to the repetition rate of 85.91 kHz. It is observed that the generated pulses are stable without any amplitude modulation. This indicates that there is no self-mode locking (SML) impact during the Q-switching operation.

Inset of Figure 4.5(c) shows a single pulse envelope showing a uniform shape with a pulse width of approximately 4.66 µs. To verify that ZnO PMMA SA attributed to the generation of passive Q-switched, the SA film is detaching from the EDFL cavity. Based on the observation from an oscilloscope, as the pump power being adjusted up to the maximum pump power, which is 200 mW, no Q-switched pulses were detected. This finding confirmed that the ZnO PMMA film was responsible for the passively Q-switched operation of the laser.

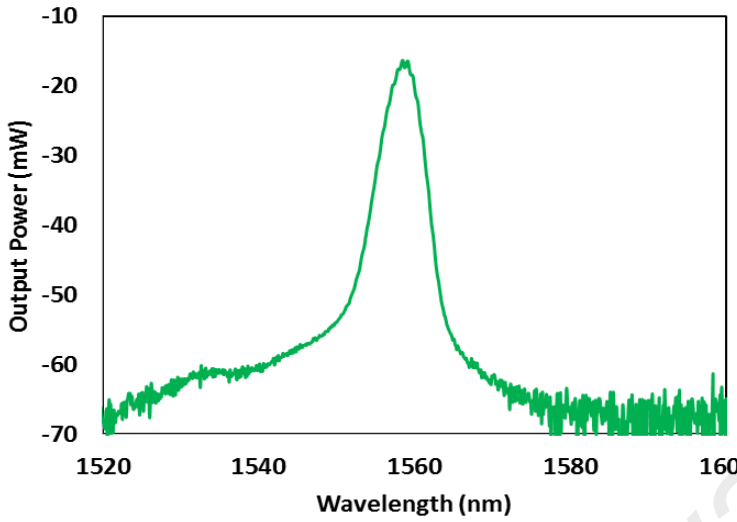

(a)

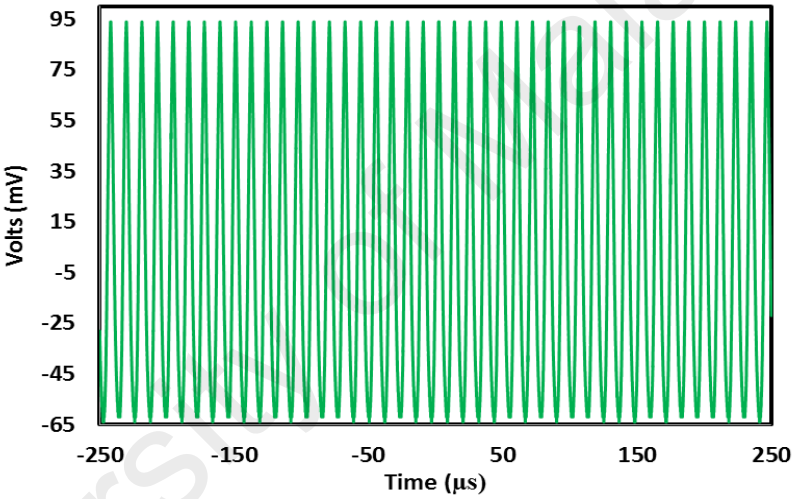

(b)

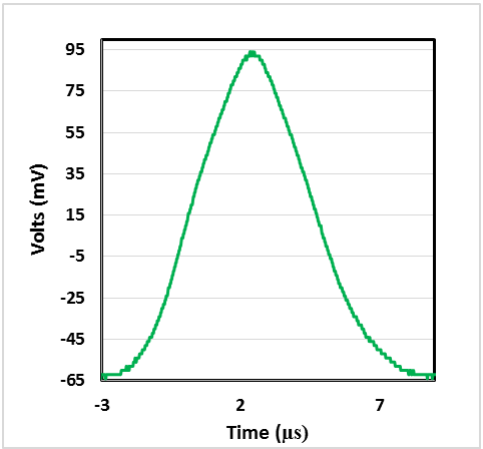

(c)

Figure 4.5: Pulse characteristic at a pump power of 98.49 mW, showing (a) the pulse wavelength spectrum, (b) the typical pulse train and (c) a single envelops of the pulse.

During the process of increasing pump powers, the stable repetition rate of output pulse is monotonically increasing from 24.85 kHz to 85.91 kHz while the pulse duration reduces from 17.88 µs to 4.66 µs as shown in Figure 4.6. A distinctive characteristic of passive Q-switched laser is shown in the result. As the pump power is continuously being an increase, the upper level of the pump rate become increases and causes the increase of the repetition rate and the reduction of the pulse width (Jiang et al., 2012; Zhou, Wei, Dong, & Liu, 2010). The demonstrated laser shows no obvious degradation at the laboratory condition for two hours. In our experiment, no stable pulse trains are observed when the pump power goes beyond 98.49 mW. The laser becomes CW operation when the pump power rises from 98.49 mW to 200 mW. If the pump power is reduced to 98.49 mW again, the Q-switching reappeared. This is because ZnO PMMA SA exhibits a saturable absorption at moderate laser intensities, while optical limiting induced by excited states absorption would occur at higher intensities (Bai et al., 2016; Mary et al., 2011; Nair, Thomas, Suchand Sandeep, Anantharaman, & Philip, 2008; Xing, Jiang, Ying, & Ji, 2010).

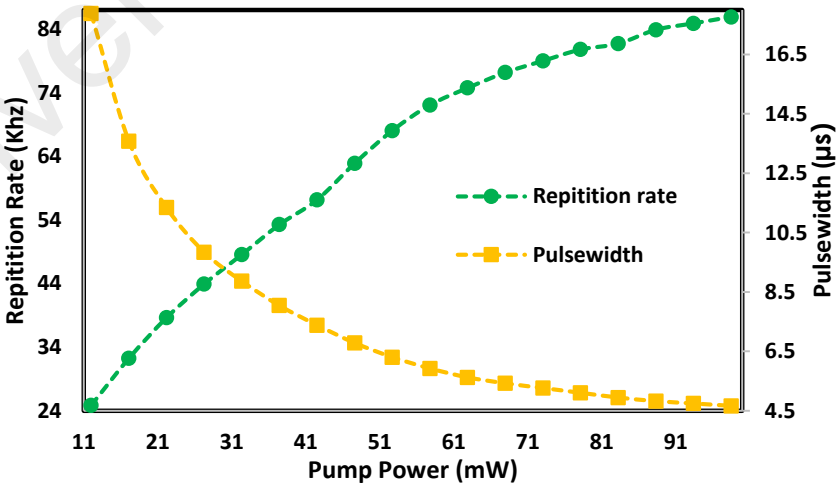

Figure 4.6: Repetition rate and pulse width against the pump power for the Q-switched EDFL with ZnO PMMA film

Figure 4.7 indicates a relationship between pulse energy and the average output power against the pump power. A typical Q-switching behaviour can be obtained as the SA saturate from an addition of the gain. When the pump increased its power to a range of 12 mW to 98.49 mW, the average output power had been rising from 0.88 mW to 9.96 mW. Therefore, the output power and pump power relationship can be fitted with y=0.1048x-0.0914, and the corresponding fitting coefficient R^2 is 0.9971. Besides that, the laser efficiency obtained in this experiment is about 10.5 %. Pulse energy also is discovered to be changed while a pump power is increased. Single pulse energy has been varied in a range of 35.45 nJ to 115.94 nJ when the power of the pump is increased from 12 to 98.49 mW. An increment of the pump power has led to a rise of average output power while shortening a pulse width and hence higher pulse energy is extracted in the Q-switching process. To investigate the stability of our Q-switched pulse, the radiofrequency (RF) spectrum is obtained at the pump power of 98.49 mW, as illustrated in Figure 4.8. The RF spectrum shows the fundamental frequency of 85.91 kHz with a high signal to noise ratio (SNR) of 67.1 dB. The SNR in the ZnO PMMA indicates a better pulse train stability, comparable to the Q-switched fibre lasers SA establish from CNT and graphene (Ahmad et al., 2013; M. Ahmed et al., 2015; S. Harun et al., 2012)

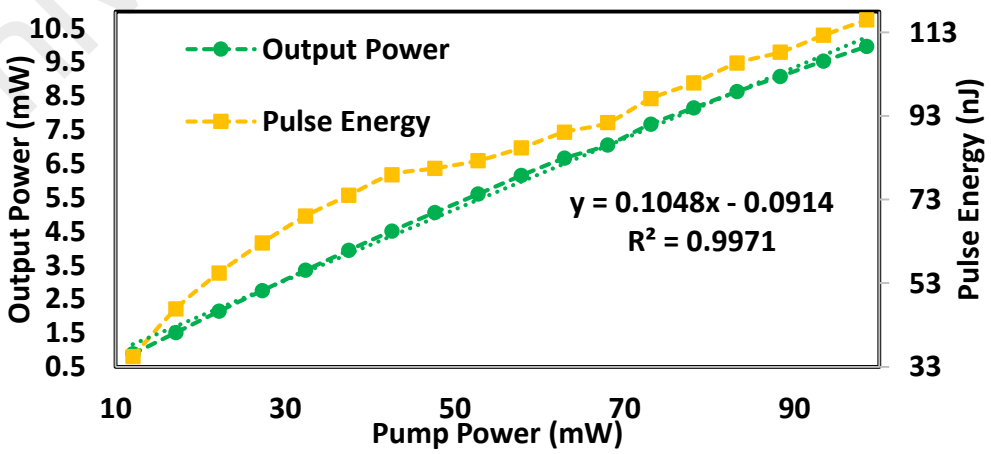

Figure 4.7: Output power and pulse energy against the pump power for the Q-switched EDFL with ZnO PMMA film

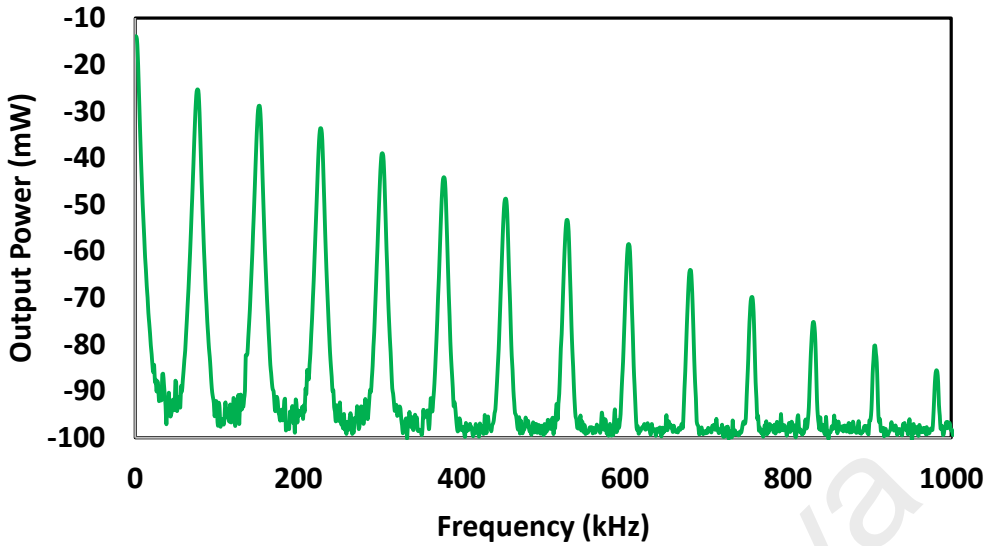

Figure 4.8: The output pulse spectrum in the frequency domain for the Q-switched EDFL with ZnO PMMA film at pump power of 98.49 mW.

The cavity laser then was left to continuously operate for 48 hours and based on observation, the Q-switching pulses are excessively firm without any significant changes in any of the output parameters. During the operation, pump power is being increased up to 200mW and it was found that the ZnO PMMA SA was not affected by the high power. This shows that the thermal damage threshold for the SA is above 200 mW pump power. For a Q-switched fibre laser, a lower repetition rate and pump power are preferred because the intra-cavity power can be more effectively coupled to each pulse at this situation to achieve higher pulse energy. Even though current pulse energy is unable to perform better than a laser with a conventional semiconductor-based SAs, a better enhancement to scaling up the pulse energy is predictable with ZnO-based SA by optimizing the fabrication procedure.

4.5 Q-switching Performance with ZnO PVA film

4.5.1 ZnO PVA thin film Characteristic

In this section, a Q-switched EDFL is demonstrated using a ZnO PVA SA as a Q-switcher. At first, the ZnO PVA film was fabricated as described in section 4.2. We verify the quality of the ZnO PVA film by using Field Emission Scanning Electron Microscopy **(**FESEM**)** as present in Figure. 4.9 (a). The FESEM image indicates the existence of the unvarying layers and confirms the absence of > 1μm aggregates or voids in the composite SA, which otherwise result in non-saturable scattering losses.

The inset of Figure 4.9 (b) shows the physical thin film as viewed normally. The thin film's thickness was measured to be approximately 50 μm. We cut a small piece of the ZnO film and attached it onto a standard FC/PC fibre ferrule end surface with index matching gel. After connecting it with another FC/PC fibre ferrule with a standard flange adapter, the all-fibre ZnO based SA was finally ready.

Other than FESEM, ZnO PVA film also undergoes a test to investigate the absorption amount for a various input intensities to determine a nonlinear saturable absorption property. The result is indicated in Figure 4.10. Based on the observation in the curve of the graph, the nonsaturable absorption, modulation depth and the saturation intensity of the film are estimated to be around 4 %, 5 %, and 60 MW/cm^2 respectively. Since ZnO response in a nonlinear optical where it is possible to guide a relatively low fluence to absorb the laser until it saturates, therefore, ZnO film has been determining to be a potential material to work as a passive SA in a fibre laser set up.

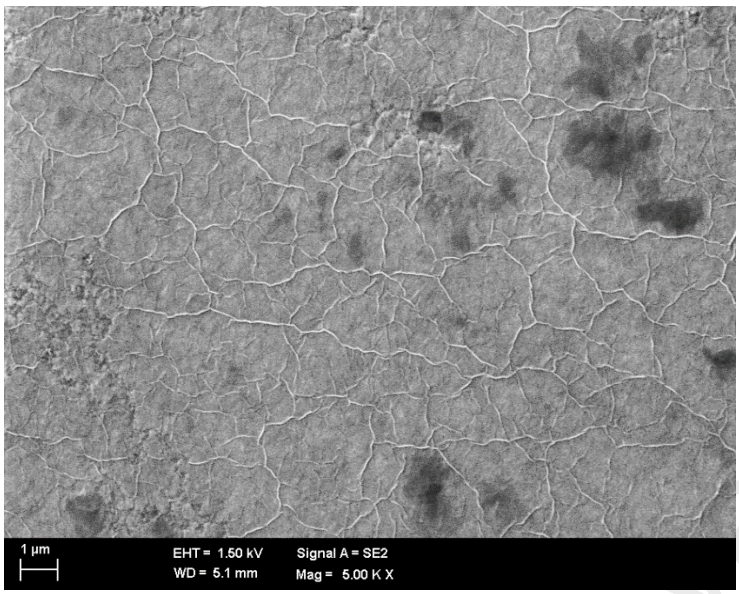

(a)

(b)

Figure 4.9: Image capture of ZnO (a) FESEM (b) Actual film, as viewed without any magnification

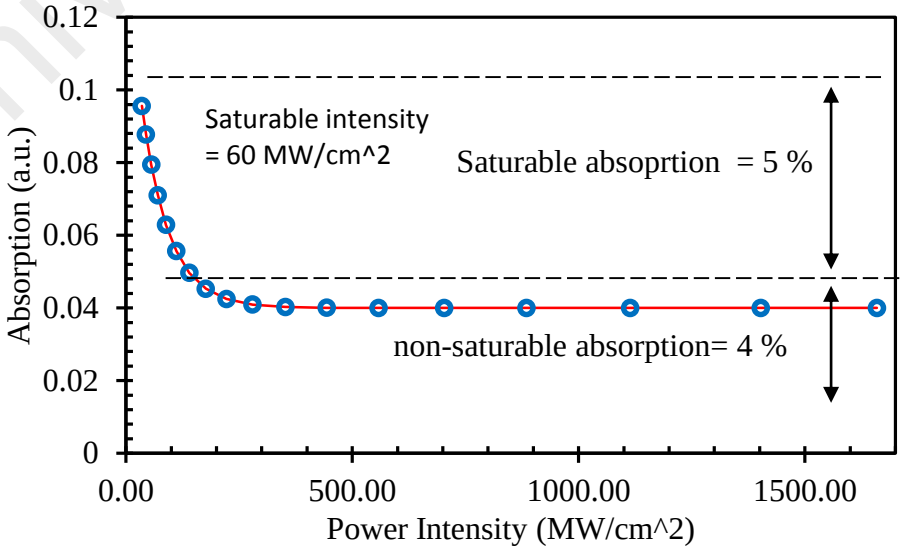

Figure 4.10: Nonlinear absorption curve for the ZnO PVA film

4.5.2 Result and Discussion

The fabricated SA device is incorporated in an EDFL cavity for Q-switching generation as described in section 4.3. In this experiment, pump power was slowly increased until we obtained a stable pulse train of the Q-switched as a pump power exceeds the lasing threshold. Stable, robust and self-starting Q-switching operation is obtained at a pump power threshold of 11.8 mW. When the pump power value is lower than the threshold, no lasing can be determining. Such a low threshold power for Q-switching operation resulted from the small intra-cavity loss performed by the ZnO PVA SA. The spectrum of the Q-switched pulse train is shown in Figure 4.11(a). It operates at 1560.4 nm with a noticeable spectral broadening as a result of a self-phase modulation of the ring cavity. A stable pulse train with an increasing repetition rate was observed within the pump power from 11.8 to 77.9 mW, which is a typical characteristic for the Q-switched laser. Figure 4.11(b) shows a typical oscilloscope trace of the Q-switched pulse train at the pump power of 77.9 mW. It shows the peak to peak duration of 16.28 μs, which is equal to the repetition rate of 61.43 kHz. It is also observed that the Q-switched pulse output was stable and no amplitude modulations in the pulse train were found, which indicates that there was no self-mode locking (SML) effect during the Q-switching operation. A single Q-switched pulse is shown in Figure 4.11(c) which has an almost symmetric shape with a pulse width of approximately 7.0 μs. To verify that the passive Q-switching was attributed to the ZnO PVA SA, the film was removed from the ring cavity. In this case, no Q-switched pulses were observed on the oscilloscope even when the pump power was adjusted over a wide range. This finding confirmed that the ZnO PVA SA was responsible for the passively Q-switched operation of the laser.

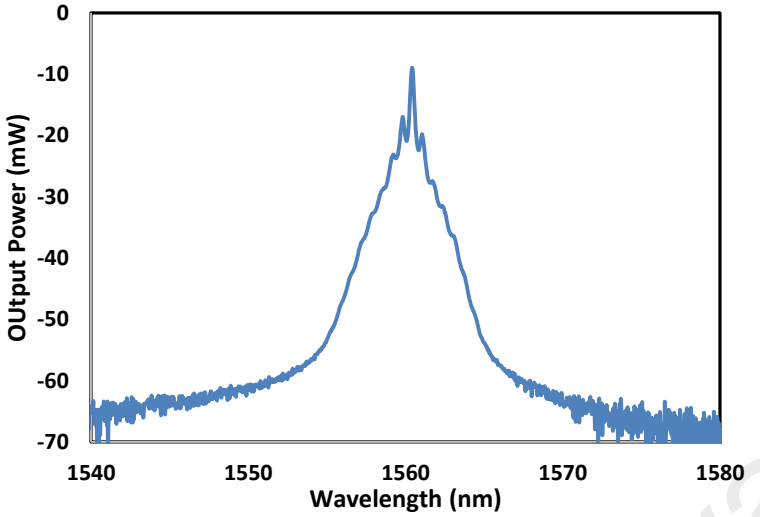

(a)

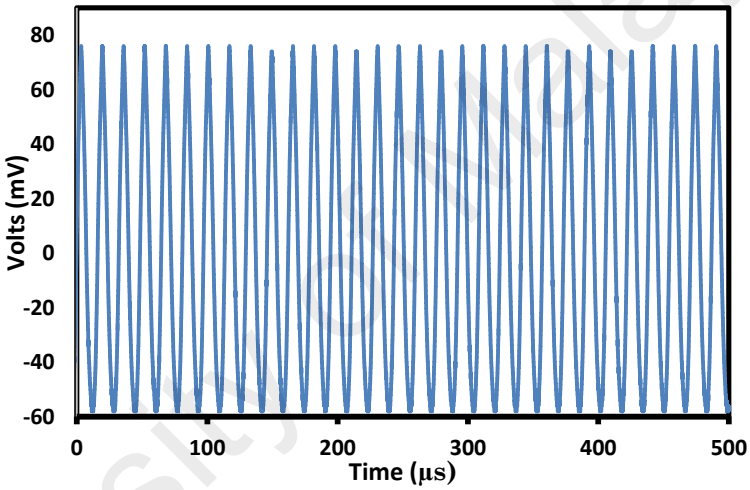

(b)

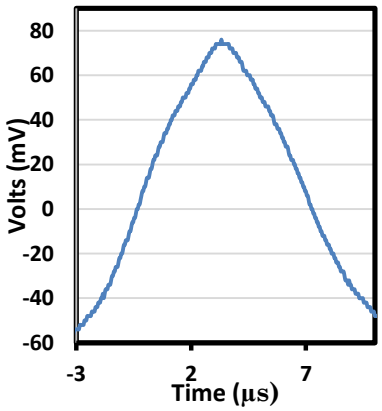

(c)

Figure 4.11: Pulse characteristic at a pump power of 77.9 mW, showing (a) the pulse wavelength spectrum, (b) the typical pulse train and (c) a single envelops of the pulse.

In Figure 4.12, we show the pulse repetition rate and the pulse duration as a function of pump power. It is clear that with increasing pump power from 11.8 mW to 77.9 mW, the repetition rate grows monotonously from 22.79 to 61.43 kHz. The pulse repetition rate increases almost linearly with the pump power at the rate of ~0.56 kHz/mW. On the other hand, the pulse duration decreases from 20.36 - 7.00 μs with the increase of the pump power from the threshold of 11 mW to 77 mW. At lower pump power (<30 mW), the pulse duration drops exponentially. At higher pump power (>30 mW) the pulse duration linearly reduces while the repetition rate increases. As pump power increases, more power circulates inside the laser cavity, thus hasten the saturation of SA. From Figure 4.12 it can be seen that smaller changes of pulse width from 30-77 mW indicate the SA was becoming saturated with continually increasing the light intensity (pump power). It is also worthy to note that pulse operation was switched into CW mode as the pump increased above than 77 mW. The pulse duration can be further decreased by shortening the length of the laser cavity (including the length of the gain material), but this would compromise the optical output.

Figure 4.13 shows the dependence of the pulse energy and the average output power of the laser against the pump power. The average output power increases linearly with the pump power with a slope efficiency of 13%. The pulse energy also increases monotonously with the pump power where the maximum pulse energy of 154.6 nJ is obtained at the pump power of 77 mW. The increment of pump power leads to a rise of average output power and shorten the pulse width, and hence higher pulse energy is extracted in the Q-switching process. Compared to the previous carbon nanotubes (S. Harun et al., 2012) and graphene (Yap et al., 2012) based Q-switching, the attainable pulse energy is higher. The ZnO SA was also tested in Ytterbium-doped fibre laser, and Thulium-doped fibre laser cavity and the almost similar Q-switching performance was

also realised. This showed that the proposed ZnO SA could operate in wide wavelength region ranging from 1.0 to 2.0 μm.

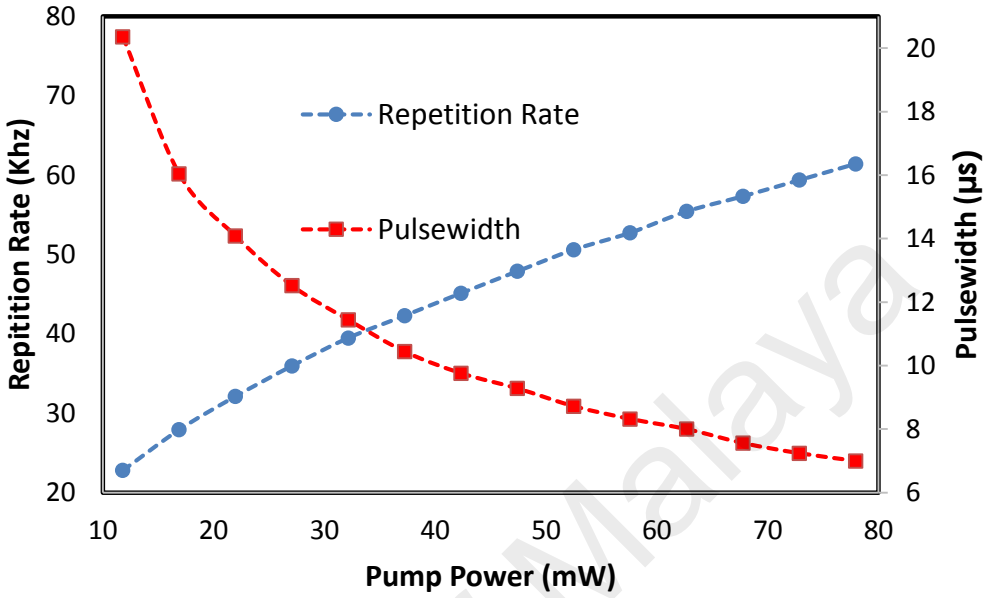

Figure 4.12: The pulse repetition rate and the pulse duration as a function of pump power

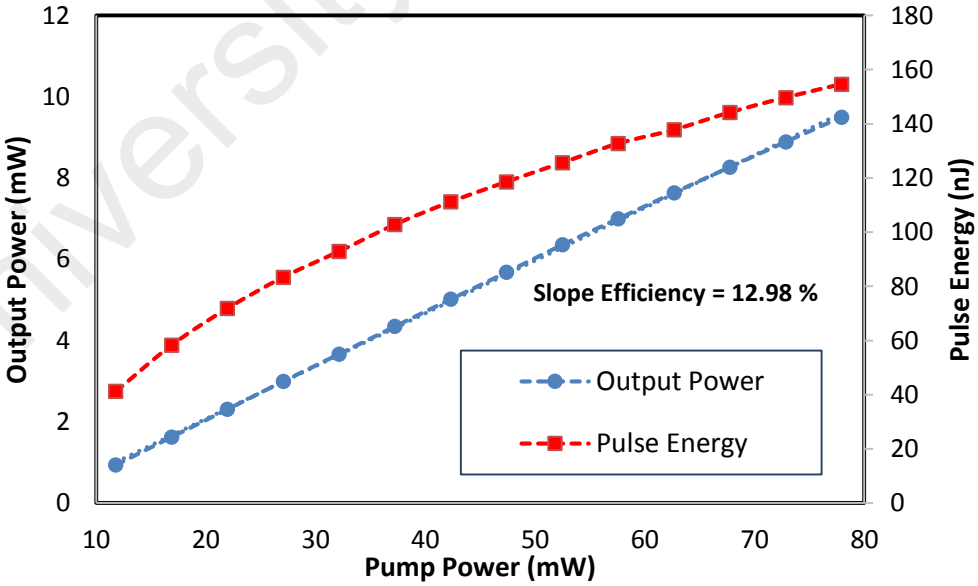

Figure 4.13: The pulse average output power and energy as a function of pump power.

To investigate the stability of our Q-switched pulse, the radio-frequency (RF) spectrum is obtained at the pump power of 77.9 mW as shown in Figure 4.14. The RF spectrum shows the fundamental frequency of 64.43 kHz with a high signal to noise ratio (SNR) of ~62 dB. The SNR indicates good pulse train stability, comparable to Q-switched fibre lasers based on TiO (Ahmad, Reduan, et al., 2016). The proposed laser is observed to be highly stable, with no significant changes observed in any of the output parameters after two hours of operation, and repeated cycles of operation in the two days following. The long-term stability is expected to be remarkable since the laser produced a similar output pulse train after 48 hours of operation. It is expected that a better Q-switched pulse can be obtained by optimizing the design of the cavity, including reducing the cavity length and cavity losses as well as optimizing its cavity structure and using higher quality ZnO based SAs.

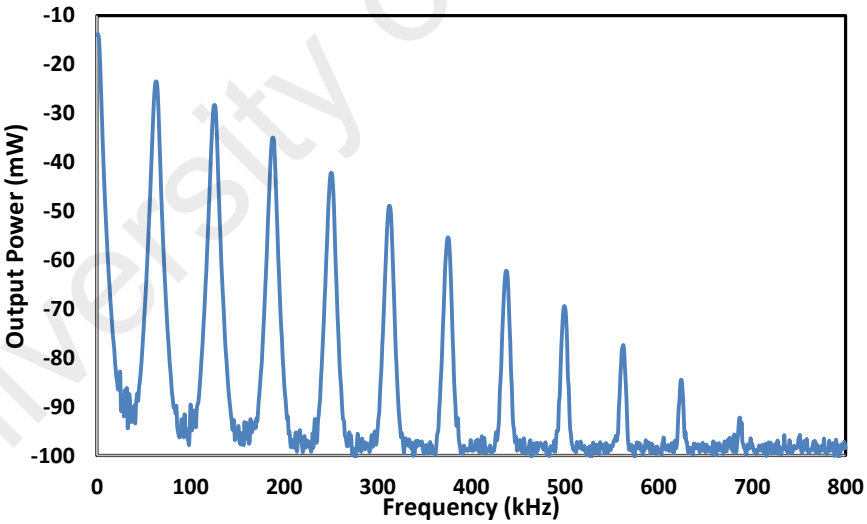

Figure 4.14: The output pulse spectrum in the frequency domain at a pump power of 77.9 mW

4.6 Summary

A Q-switched ring EDFL was successfully demonstrated using a ZnO powder, which is embedded into a PMMA and PVA films as a passive SA. The film with about 50 μm thickness was sandwiched between two ferrules via a fibre connector to form a fibre-compatible SA. With a ZnO PMMA film, stable passively Q-switched EDFL pulses operating at 1559.3 nm with a maximum output pulse energy of 115.93 nJ, the repetition rate of 85.91 kHz, and pulse width of 4.66 μs are achieved when the input pump power is 98.49 mW at the wavelength of 980 nm. The laser features a low threshold pump power of ~12 mW. As the SA device is changed to ZnO PVA film, stable Q-switched pulses train at 1560.4 nm was also successfully obtained within the 980nm pump power range from 11.8 mW to 77.9 mW. At 77.9 mW pump power, the laser showed the repetition rate, pulse energy, and pulse duration of 61.43 kHz, 154.6 nJ, and 7.00 μs, respectively. With PVA film, the maximum attainable pulse energy is improved. These results show that ZnO is a new potential SA material for pulsed laser applications. Both Q-switched lasers feature a low threshold due to tremendous third-order optical response with a fast response time for the ZnO-based SA. The facile fabrication, excellent stability and robust structure of ZnO-based SA will facilitate many more potential nonlinear photonic applications, which are expected to work towards ultrafast photonics and play a key role in other nonlinear photonics applications.

CHAPTER 5:

CONCLUSION AND FUTURE WORK

Passively Q-switched fibre lasers had gained much attention due to their potentials as compact, simple, flexible, stable sources in medicine, laser processing, telecommunications, and remote sensing. They had been investigated intensively using different kinds of saturable absorbers (SAs) while many methods and new materials were explored. The research work aims to demonstrate Q-switched EDFL using two types of nanomaterials as SAs; graphene oxide (GO) and zinc oxide (ZnO). The SA device was fabricated by embedding these materials into two types of polymer which is PVA and PMMA film. Stable and high-power Q-switching pulses were obtained by incorporating a small piece of the film in an EDFL cavity.

Q-switched EDFLs have been successfully demonstrated based on the newly developed GO film based SAs. Due to its unselective absorption, the graphene-based SA can operate in a broad wavelength range. The SA devices were successfully fabricated by embedding a GO material, which was obtained through chemical oxidation of graphite into both PMMA and PVA polymers. A stable Q-switched pulse which operates at 1531.6 nm was successfully generated by incorporating the prepared GO PMMA SA into an EDFL cavity. By increasing the pump power within a range of 11.8 to 83.0 mW, the repetition rate of the laser could be increased from 21.5 kHz to 68.7 kHz, and pulse duration could be reduced from 20.44 μs to 6.12 μs. At the maximum pump power of 83.00 mW, the pulse energy of 145 nJ was achieved.

By replacing the SA device to GO PVA film-based device, the EDFL also generates a stable Q-switching pulse train that is able to operate at a longer wavelength of 1560.5 nm. With the GO PVA SA, the Q-switched was realised at a higher pump power threshold of 16.88 mW and the Q-switching operation was maintained up to 72.85 mW

pump power. By gradually raising the pump power within the range, the repetition rate has risen from 32.45 kHz to 81.7 kHz while the pulse width dropped from 14.28 µs to 5.67 µs. At the maximum pump of 72.85 mW, the highest repetition rate and single pulse energy of 81.7 kHz and 109.30 nJ were achieved. These results show that GO PMMA film has a better performance compared to the PVA film in terms of the pulse energy and range of the operating pump power.

Later, two Q-switched EDFLs were also proposed and shown using a ZnO based SA. At first, the SA is fabricated by embedding a prepared ZnO powder into PMMA film. The film, which has a thickness of approximately 50 µm was sandwiched between two ferrules through a fibre connector in order to form a fibre-compatible SA. The proposed laser generated a stable Q-switched pulses train by incorporating the SA film in the laser cavity, where the repetition rate rises from 24.85 to 85.91 kHz while the pulse width reduces from 17.88 to 4.66 µs as the pump power rose from 12 to 98.49 mW. The Q-switched laser operated at 1559.3 nm with the maximum output pulse energy of 115.93 nJ while featuring a low threshold pump power of ~12 mW. It is worthy to note that the EDFL generates a stable Q-switched pulses trained with a higher pulses energy when the polymer material was replaced from PMMA to PVA.

As the SA device is changed to ZnO PVA film, the laser operated at 1560.4 nm within the 980nm pump power range from 11.8 mW to 77.9 mW. At 77.9 mW pump power, the repetition rate, pulse energy, and pulse duration generated by the proposed lasers were 61.43 kHz, 154.6 nJ, and 7.00 µs, respectively. Thus, these findings revealed that both GO and ZnO materials have new potentials for applications in pulsed laser generation. Both Q-switched lasers feature a low threshold because of its large third-order optical response with a fast response time for the ZnO-based SA. Since ZnO-based SA is easy to fabricate, has a good stability as well as having a robust structure, it will be

beneficial to numerous potential nonlinear photonic applications, in particular, ultrafast photonics and plays a key role in other nonlinear photonics applications.

There are several aspects that need to be considerate for further improvements. First, would be by further optimizing of the laser cavity to achieve mode-locking operation. Future studies should also be focusing on exploring more on the optical properties of both GO and ZnO SA for ultrafast laser generation. Fibre lasers have low repetition rate due to the relatively long length of the cavity. However, for various applications such as communications and for quantum experiments, the high repetition rate is desirable. Currently, harmonic mode-locking is the most promising way to generate high repetition rates. Future efforts will be focused on the theory of high-repetition rate mode-locked cavities or harmonic mode-locking and experimentally developing a very stable passive harmonic mode-locked EDFL by manipulating the laser cavity.

REFERENCES

Adel, P., Auerbach, M., Fallnich, C., Unger, S., Müller, H.-R., & Kirchhof, J. (2003). Passive Q-switching by Tm 3+ co-doping of a Yb 3+-fibre laser. *Optics express, 11*(21), 2730-2735.

Ahmad, H., Lee, C., Ismail, M., Ali, Z., Reduan, S., Ruslan, N., . . . Harun, S. (2016). Zinc oxide (ZnO) nanoparticles as saturable absorber in passively Q-switched fibre laser. *Optics Communications, 381,* 72-76.

Ahmad, H., Muhammad, F., Zulkifli, M., & Harun, S. (2013). Q-switched pulse generation from an all-f iber distributed Bragg reflector laser using graphene as saturable absorber. *Chinese Optics Letters, 11*(7), 071401.

Ahmad, H., Reduan, S. A., Ali, Z. A., Ismail, M., Ruslan, N., Lee, C., . . . Harun, S. (2016). C-Band Q-Switched Fibre Laser Using Titanium Dioxide (TiO 2) As Saturable Absorber. *IEEE Photonics Journal, 8*(1), 1-7.

Ahmed, M., Ali, N., Salleh, Z., Rahman, A., Harun, S., Manaf, M., & Arof, H. (2015). Q-switched erbium doped fibre laser based on single and multiple walled carbon nanotubes embedded in polyethylene oxide film as saturable absorber. *Optics & Laser Technology, 65*, 25-28.

Ahmed, M. H. M. (2015). *Development of Q-Switched and Mode-locked Erbium Doped Fibre Lasers Based on Carbon Nanotubes Saturable Absorbers.* Jabatan Kejuruteraan Elektrik, Fakulti Kejuruteraan, Universiti Malaya,

Ahmed, M. H. M., Ali, N. M., Salleh, Z. S., Rahman, A. A., Harun, S. W., Manaf, M., & Arof, H. (2015). Q-switched erbium doped fibre laser based on single and multiple walled carbon nanotubes embedded in polyethylene oxide film as saturable absorber. *Optics and Laser Technology, 65*, 25-28. doi:10.1016/j.optlastec.2014.07.001

Alvarez-Chavez, J. A., Offerhaus, H. L., Nilsson, J., Turner, P., Clarkson, W., & Richardson, D. (2000). High-energy, high-power ytterbium-doped Q-switched fibre laser. *Optics Letters, 25*(1), 37-39.

Aneesh, P., Vanaja, K., & Jayaraj, M. (2007). *Synthesis of ZnO nanoparticles by hydrothermal method.* Paper presented at the Proc. SPIE.

Antipov, O. L., Zakharov, N. G., Fedorov, M., Shakhova, N. M., Prodanets, N. N., Snopova, L. B., . . . Sroka, R. (2011). Cutting effects induced by 2μm laser radiation of cw Tm: YLF and cw and Q-switched Ho: YAG lasers on ex-vivo tissue. *Medical Laser Application, 26*(2), 67-75.

Bagnall, D., Chen, Y., Zhu, Z., Yao, T., Koyama, S., Shen, M. Y., & Goto, T. (1997). Optically pumped lasing of ZnO at room temperature. *Applied Physics Letters, 70*(17), 2230-2232.

Bai, X., Mou, C., Xu, L., Wang, S., Pu, S., & Zeng, X. (2016). Passively Q-switched erbium-doped fibre laser using Fe3O4-nanoparticle saturable absorber. *Applied Physics Express, 9*(4), 042701.

Bao, Q. L., Zhang, H., Wang, Y., Ni, Z. H., Yan, Y. L., Shen, Z. X., . . . Tang, D. Y. (2009). Atomic-Layer Graphene as a Saturable Absorber for Ultrafast Pulsed Lasers. *Advanced Functional Materials, 19*(19), 3077-3083. doi:10.1002/adfm.200901007

Becker, P. C., Olsson, A. N., & Simpson, J. R. (1999). *Erbium-doped fibre amplifiers: fundamentals and technology*: Academic press.

Bello-Jimenez, M., Cuadrado-Laborde, C., Saez-Rodriguez, D., Diez, A., Cruz, J. L., & Andres, M. V. (2010). Actively mode-locked fibre ring laser by intermodal acousto-optic modulation. *Optics Letters, 35*(22), 3781-3783. doi:10.1364/ol.35.003781

Boguslawski, J., Sotor, J., Sobon, G., Kozinski, R., Librant, K., Aksienionek, M., . . . Abramski, K. M. (2015). Graphene oxide paper as a saturable absorber for Er- and Tm-doped fibre lasers. *Photonics Research, 3*(4), 119-124. doi:10.1364/prj.3.000119

Bose, S., & Barua, A. (1999). The role of ZnO: Al films in the performance of amorphous-silicon based tandem solar cells. *Journal of Physics D: Applied Physics, 32*(3), 213.

Bouma, B. E., Nelson, L. E., Tearney, G. J., Jones, D. J., Brezinski, M. E., & Fujimoto, J. G. (1998). Optical coherence tomographic imaging of human tissue at 1.55 μm and 1.81 μm using Er-and Tm-doped fibre sources. *Journal of Biomedical Optics, 3*(1), 76-79.

Chandonnet, A., & Larose, G. (1993). High-power Q-switched erbium fibre laser using an all-fibre intensity modulator. *Optical engineering, 32*(9), 2031.

Chen, Y., Xi, J., Dumcenco, D. O., Liu, Z., Suenaga, K., Wang, D., . . . Xie, L. (2013). Tunable band gap photoluminescence from atomically thin transition-metal dichalcogenide alloys. *Acs Nano, 7*(5), 4610-4616.

Coleman, V., & Jagadish, C. (2006). Basic properties and applications of ZnO. *Zinc Oxide Bulk, Thin Films and Nanostructures: Processing, Properties, and Applications*, 1-20.

De Tan, W., Tang, D., Xu, X., Zhang, J., Xu, C., Xu, F., . . . Xu, J. (2010). Passive femtosecond mode-locking and cw laser performance of Yb 3+: Sc 2 SiO 5. *Optics express, 18*(16), 16739-16744.

Delgado-Pinar, M., Zalvidea, D., Diez, A., Pérez-Millán, P., & Andrés, M. (2006). Q-switching of an all-fibre laser by acousto-optic modulation of a fibre Bragg grating. *Optics express, 14*(3), 1106-1112.

Delgado-Pinar, M., Zalvidea, D., Diez, A., Perez-Millan, P., & Andres, M. V. (2006). Q-switching of an all-fibre laser by acousto-optic modulation of a fibre Bragg grating. *Optics express, 14*(3), 1106-1112. doi:10.1364/oe.14.001106

Desurvire, E., Giles, C. R., Simpson, J. R., & Zyskind, J. L. (1991). Erbium-doped fibre amplifier. In: Google Patents.

Dong, L., & Samson, B. (2016). *Fibre Lasers: Basics, Technology, and Applications*: Crc Press.

Dvoyrin, V. V., Mashinsky, V. M., & Dianov, E. (2007). Yb-Bi pulsed fibre lasers. *Optics Letters, 32*(5), 451-453.

El-Mashade, M. B., & Mohamed, A. (2017). Characteristics Evaluation of Multi-Stage Optical Amplifier EDFA. *British journal of Applied Science & Technology, 19(4): 1-20, 2017*(31911).

Fan, D., Mou, C., Bai, X., Wang, S., Chen, N., & Zeng, X. (2014). Passively Q-switched erbium-doped fibre laser using evanescent field interaction with gold-nanosphere based saturable absorber. *Optics express, 22*(15), 18537-18542.

Fermann, M. E., Galvanauskas, A., & Sucha, G. (2002). *Ultrafast lasers: Technology and applications* (Vol. 80): CRC Press.

Ferrari, A. C., & Robertson, J. (2000). Interpretation of Raman spectra of disordered and amorphous carbon. *Physical Review B, 61*(20), 14095-14107. doi:10.1103/PhysRevB.61.14095

Fotiadi, A., Deparis, O., Kiyan, R., Chernikov, S., & Ikiades, A. (2000). *Passive Q-switching dynamics in SBS/Er fibre laser at low pump power*. Paper presented at the Lasers and Electro-Optics Society 2000 Annual Meeting. LEOS 2000. 13th Annual Meeting. IEEE.

Graphene-Info. (2017). *Graphene Oxide: Introduction and Market News.* Retrieved from http://www.graphene-info.com/graphene-oxide

Haripadmam, P., John, H., Philip, R., & Gopinath, P. (2014). Switching of absorptive nonlinearity from reverse saturation to saturation in polymer-ZnO nanotop composite films. *Applied Physics Letters, 105*(22), 221102.

Harun, S., Ismail, M., Ahmad, F., Ismail, M., Nor, R., Zulkepely, N., & Ahmad, H. (2012). A Q-switched erbium-doped fibre laser with a carbon nanotube based saturable absorber. *Chinese physics letters, 29*(11), 114202.

Harun, S. W., Ismail, M. A., Ahmad, F., Ismail, M. F., Nor, R. M., Zulkepely, N. R., & Ahmad, H. (2012). A Q-Switched Erbium-Doped Fibre Laser with a Carbon Nanotube Based Saturable Absorber. *Chinese physics letters, 29*(11), 3. doi:10.1088/0256-307x/29/11/114202

Hasan, T., Sun, Z., Wang, F., Bonaccorso, F., Tan, P. H., Rozhin, A. G., & Ferrari, A. C. (2009). Nanotube–polymer composites for ultrafast photonics. *Advanced Materials, 21*(38- 39), 3874-3899.

Hassan, N. K., Hashim, M. R., & Al-Douri, Y. (2014). Morphology and optical investigations of ZnO pyramids and nanoflakes for optoelectronic applications. *Optik, 125*(11), 2560-2564. doi:10.1016/j.ijleo.2013.10.023

Henderson, S. W., Suni, P. J., Hale, C. P., Hannon, S. M., Magee, J. R., Bruns, D. L., & Yuen, E. H. (1993). Coherent laser radar at 2 mu m using solid-state lasers. *IEEE transactions on geoscience and remote sensing, 31*(1), 4-15.

Hendow, S. T., & Shakir, S. A. (2010). Structuring materials with nanosecond laser pulses. *Optics express, 18*(10), 10188-10199.

Hisamuddin, N., Zakaria, U., Zulkifli, M., Latiff, A., Ahmad, H., & Harun, S. (2016). Q-Switched Raman Fibre Laser with Molybdenum Disulfide-Based Passive Saturable Absorber. *Chinese physics letters, 33*(7), 074208.

Hisyam, M. B., Rusdi, M. F., Latiff, A. A., & Harun, S. W. (2016). PMMA-doped CdSe quantum dots as saturable absorber in a Q-switched all-fibre laser. *Chinese Optics Letters, 14*(8), 5. doi:10.3788/col201614.081404

Huang, D.-W., Liu, W.-F., & Yang, C. (2000). Q-switched all-fibre laser with an acoustically modulated fibre attenuator. *IEEE Photonics technology letters, 12*(9), 1153-1155.

Jagadish, C., & Pearton, S. J. (2011). *Zinc oxide bulk, thin films and nanostructures: processing, properties, and applications*: Elsevier.

Jamdagni, P., Khatri, P., & Rana, J. (2016). Green synthesis of zinc oxide nanoparticles using flower extract of Nyctanthes arbor-tristis and their antifungal activity. *Journal of King Saud University-Science*.

Janotti, A., & Van de Walle, C. G. (2009). Fundamentals of zinc oxide as a semiconductor. *Reports on progress in physics, 72*(12), 126501.

Jiang, T., Xu, Y., Tian, Q., Liu, L., Kang, Z., Yang, R., . . . Qin, W. (2012). Passively Q-switching induced by gold nanocrystals. *Applied Physics Letters, 101*(15), 151122.

Jimenez-Garcia, F. N., Londono-Calderon, C. L., Espinosa-Arbelaez, D., Del Real, A., & Rodriguez-Garcia, M. (2014). Influence of substrate on structural, morphological and optical properties of ZnO films grown by SILAR method. *Bulletin of Materials Science, 37*(6), 1283-1291. doi:10.1007/s12034-014-0073-7

Johnson, J. C., Knutsen, K. P., Yan, H., Law, M., Zhang, Y., Yang, P., & Saykally, R. J. (2004). Ultrafast carrier dynamics in single ZnO nanowire and nanoribbon lasers. *Nano Letters, 4*(2), 197-204.

Keller, U. (2003). Recent developments in compact ultrafast lasers. *Nature, 424*(6950), 831-838.

Keller, U., Weingarten, K. J., Kartner, F. X., Kopf, D., Braun, B., Jung, I. D., . . . Der Au, J. A. (1996). Semiconductor saturable absorber mirrors (SESAM's) for

femtosecond to nanosecond pulse generation in solid-state lasers. *IEEE Journal of Selected Topics in Quantum Electronics, 2*(3), 435-453.

Kezirian, G. M., & Stonecipher, K. G. (2004). Comparison of the IntraLase femtosecond laser and mechanical keratomes for laser in situ keratomileusis. *Journal of Cataract & Refractive Surgery, 30*(4), 804-811.

Kozinc, M. (2015). Pulsed Solid State Laser with Passive Q-switch. In: February.

Kudin, K. N., Ozbas, B., Schniepp, H. C., Prud'homme, R. K., Aksay, I. A., & Car, R. (2008). Raman spectra of graphite oxide and functionalized graphene sheets. *Nano Letters, 8*(1), 36-41. doi:10.1021/nl071822y

Laming, R., Farries, M., Morkel, P., Reekie, L., Payne, D., Scrivener, P., . . . Righetti, A. (1989). Efficient pump wavelengths of erbium-doped fibre optical amplifier. *Electronics Letters, 25*(1), 12-14.

Lin, J.-H., Chen, Y.-J., Lin, H.-Y., & Hsieh, W.-F. (2005). Two-photon resonance assisted huge nonlinear refraction and absorption in ZnO thin films. *Journal of Applied Physics, 97*(3), 033526.

Liu, J., Wang, Q., & Wang, P. (2012). High average power picosecond pulse generation from a thulium-doped all-fibre MOPA system. *Optics express, 20*(20), 22442-22447.

Martinez, A., & Yamashita, S. (2011). Carbon nanotube-based photonic devices: Applications in nonlinear optics. In *Carbon Nanotubes Applications on Electron Devices*: InTech.

Mary, A. R., Sandeep, C. S., Narayanan, T., Philip, R., Moloney, P., Ajayan, P., & Anantharaman, M. (2011). Nonlinear and magneto-optical transmission studies on magnetic nanofluids of non-interacting metallic nickel nanoparticles. *Nanotechnology, 22*(37), 375702.

Mears, R. J., Reekie, L., Jauncey, I., & Payne, D. N. (1987). Low-noise erbium-doped fibre amplifier operating at 1.54 μm. *Electronics Letters, 23*(19), 1026-1028.

Mizrahi, V., DiGiovanni, D. J., Atkins, R. M., Grubb, S. G., Park, Y.-K., & Delavaux, J.-M. (1993). Stable single-mode erbium fibre-grating laser for digital communication. *Journal of Lightwave technology, 11*(12), 2021-2025.

Nair, S. S., Thomas, J., Suchand Sandeep, C., Anantharaman, M., & Philip, R. (2008). An optical limiter based on ferrofluids. *Applied Physics Letters, 92*(17), 171908.

Ngo, N. Q. (2010). *Ultra-fast fibre lasers: principles and applications with MATLAB® models*: CRC Press.

Nikumb, S., Chen, Q., Li, C., Reshef, H., Zheng, H., Qiu, H., & Low, D. (2005). Precision glass machining, drilling and profile cutting by short pulse lasers. *Thin Solid Films, 477*(1), 216-221.

Pérez-Millán, P., Díez, A., Andrés, M., Zalvidea, D., & Duchowicz, R. (2005). Q-switched all-fibre laser based on magnetostriction modulation of a Bragg grating. *Optics express, 13*(13), 5046-5051.

Plamann, K., Aptel, F., Arnold, C., Courjaud, A., Crotti, C., Deloison, F., . . . Legeais, J.-M. (2010). Ultrashort pulse laser surgery of the cornea and the sclera. *Journal of Optics, 12*(8), 084002.

Reynolds, D. C., Look, D. C., & Jogai, B. (1996). Optically pumped ultraviolet lasing from ZnO. *Solid State Communications, 99*(12), 873-875.

Russo, N., Duchowicz, R., Mora, J., Cruz, J., & Andrés, M. (2002). High-efficiency Q-switched erbium fibre laser using a Bragg grating-based modulator. *Optics communications, 210*(3), 361-366.

Sangeetha, G., Rajeshwari, S., & Venckatesh, R. (2011). Green synthesis of zinc oxide nanoparticles by aloe barbadensis miller leaf extract: Structure and optical properties. *Materials Research Bulletin, 46*(12), 2560-2566.

Schmidt, A., Rivier, S., Steinmeyer, G., Yim, J. H., Cho, W. B., Lee, S., . . . Aguiló, M. (2008). Passive mode locking of Yb: KLuW using a single-walled carbon nanotube saturable absorber. *Optics Letters, 33*(7), 729-731.

Serbin, J., Bauer, T., Fallnich, C., Kasenbacher, A., & Arnold, W. (2002). Femtosecond lasers as novel tool in dental surgery. *applied surface science, 197*, 737-740.

Set, S. Y., Yaguchi, H., Tanaka, Y., & Jablonski, M. (2004). Ultrafast fibre pulsed lasers incorporating carbon nanotubes. *IEEE Journal of Selected Topics in Quantum Electronics, 10*(1), 137-146.

Shi-Xiang, X., Wen-Xue, L., Qiang, H., Hui, Z., & He-Ping, Z. (2008). Efficient laser-diode end-pumped passively Q-switched mode-locked Yb: LYSO laser based on SESAM. *Chinese physics letters, 25*(2), 548.

Shohda, F., Shirato, T., Nakazawa, M., Komatsu, K., & Kaino, T. (2008). A passively mode-locked femtosecond soliton fibre laser at 1.5 μm with a CNT-doped polycarbonate saturable absorber. *Optics express, 16*(26), 21191-21198.

Sobon, G., Sotor, J., Jagiello, J., Kozinski, R., Zdrojek, M., Holdynski, M., . . . Abramski, K. M. (2012). Graphene Oxide vs. Reduced Graphene Oxide as saturable absorbers for Er-doped passively mode-locked fibre laser. *Optics express, 20*(17), 19463-19473. doi:10.1364/oe.20.019463

Spiers, G. D., Menzies, R. T., Jacob, J., Christensen, L. E., Phillips, M. W., Choi, Y., & Browell, E. V. (2011). Atmospheric CO 2 measurements with a 2 μm airborne laser absorption spectrometer employing coherent detection. *Applied optics, 50*(14), 2098-2111.

Spiers, G. D., Menzies, R. T., Jacob, J., Christensen, L. E., Phillips, M. W., Choi, Y. H., & Browell, E. V. (2011). Atmospheric CO2 measurements with a 2 mu m airborne laser absorption spectrometer employing coherent detection. *Applied optics, 50*(14), 2098-2111. doi:10.1364/ao.50.002098

Svelto, O. (1998). Transient Laser Behavior (D. C. Hanna, Trans.). In *Principles of Lasers* (4th ed., pp. 311). New York: Springer Science+Bussiness Media.

Van Dijken, A., Meulenkamp, E., Vanmaekelbergh, D., & Meijerink, A. (2000). Identification of the transition responsible for the visible emission in ZnO using quantum size effects. *Journal of Luminescence, 90*(3), 123-128.

Wang, H. Y., Xu, W. C., Luo, A. P., Dong, J. L., Cao, W. J., & Wang, L. Y. (2012). Controllable dissipative soliton and Q-switched pulse emission in a normal dispersion fibre laser using SESAM and cavity loss tuning mechanism. *Optics communications, 285*(7), 1905-1907. doi:10.1016/j.optcom.2011.12.053

Wang, Q. H., Kalantar-Zadeh, K., Kis, A., Coleman, J. N., & Strano, M. S. (2012). Electronics and optoelectronics of two-dimensional transition metal dichalcogenides. *Nature nanotechnology*, *7*(11), 699-712.

Wang, Y., Martinez-Rios, A., & Po, H. (2003). Analysis of a Q-switched ytterbium-doped double-clad fibre laser with simultaneous mode locking. *Optics communications, 224*(1), 113-123.

Wang, Z. L. (2004). Functional oxide nanobelts: materials, properties and potential applications in nanosystems and biotechnology. *Annu. Rev. Phys. Chem., 55*, 159-196.

Wood, J. P., Plunkett, M., Previn, V., Chidlow, G., & Casson, R. J. (2011). Nanosecond pulse lasers for retinal applications. *Lasers in surgery and medicine, 43*(6), 499-510.

Xing, G., Jiang, J., Ying, J. Y., & Ji, W. (2010). Fe 3 O 4-Ag nanocomposites for optical limiting: broad temporal response and low threshold. *Optics express, 18*(6), 6183-6190.

Xu, S., & Wang, Z. L. (2011). One-dimensional ZnO nanostructures: solution growth and functional properties. *Nano Research, 4*(11), 1013-1098.

Yap, Y., Richard, M., Pua, C., Harun, S., & Ahmad, H. (2012). Graphene-based Q-switched pulsed fibre laser in a linear configuration. *Chinese Optics Letters, 10*(4), 041405.

Zhang, L., Guo, L., Xiong, B., Yan, X., Sun, L., Hou, W., . . . Li, J. (2010). LD side-pumped high beam quality passive Q-switched and mode-locked Nd: YAG laser based on SESAM. *Laser physics, 20*(9), 1798-1801.

Zhang, Z., Sang, M., Ye, Z., & Nie, Y. (2008). Passively Q- switched erbium- doped fibre laser based on nonlinear polarization rotation. *Microwave and Optical Technology Letters, 50*(3), 694-696.

Zhou, D.-P., Wei, L., Dong, B., & Liu, W.-K. (2010). Tunable passively $ Q $-switched erbium-doped fibre laser with carbon nanotubes as a saturable absorber. *IEEE Photonics technology letters, 22*(1), 9-11.

LIST OF PUBLICATIONS AND PAPERS PRESENTED

i. Aziz, N. A., Jusoh, Z., Lokman, M. Q., Yasin, M., Hanafi, E., & Harun, S. W. (2017). Q-switched erbium-doped fibre laser with graphene oxide embedded in pmma film. *Digest Journal of Nanomaterials and Biostructures*, *12*(2), 325-330.

ii. Aziz, N. A., Latiff, A. A., Lokman, M. Q., Hanafi, E., & Harun, S. W. (2017). Zinc Oxide-Based Q-Switched Erbium-Doped Fibre Laser. *Chinese Physics Letters*, *34*(4), 044202.